MASTER IN BIOLOGY OF ORGANISMS AND ECOLOGY

The influence of acclimation to density on organisms' traits and population growth in Synechococcus sp. RS 9909

Mauro, Nicola

Award date:
2024

Awarding institution:
University of Namur
Université Catholique de Louvain

Université catholique de Louvain
École de biologie

Université de Namur
Département de biologie

The influence of acclimation to density on organisms' traits and population growth in *Synechococcus* sp. RS 9909

A thesis submitted in fulfilment of the requirements for the degree of Master in Biology of Organisms and Ecology

Author : Nicola Mauro

Supervisor : Frederik De Laender (Unamur)

Academic Year 2023-2024

Acknowledgements

First, I would like to express my deep gratitude to Pr. Frederik de Laender, for his continuous guidance, valuable advice, patience, and unwavering enthusiasm throughout this experience. All these aspects helped me considerably in the realization of this project.

I would also like to thank his team, including Mark Holmes, Arunima Sikder and Camille Carpentier, for generously offering their time and assistance at every stage of the thesis development, answering my questions and guiding me whenever I needed it. Special thanks to Pauline Witsel for helping me during my initial steps in the laboratory, as well as for her support throughout the experiments, always with optimism.

I would like to thank Pr. Nicolas Schtickzelle, Pr. Alice Dennis and Lisa Buche for taking the time to review this work. In addition, I would like to thank everyone who has proofread this work to enhance its content and fluency.

Of course, I want to thank my parents, for their constant advice, help and encouragement throughout this master thesis, as well as in my daily life.

Finally, I want to thank my friends, and Sophie, for all their encouragement and support, and also for the daily moments of sharing, synonymous with joy and lightness.

Abstract

In a constantly changing environment, it is essential to understand how different factors can affect the growth of populations, including its dependence on density, commonly referred to as density dependence. These factors can affect population growth directly, by inducing a higher mortality rate for example, but also indirectly by changing organisms' traits, such as their size or their pigment content, enabling them to better cope with the changing environmental conditions in which they find themselves. This process, also known as acclimation, can have a strong influence on the density dependence of populations. It is therefore necessary, when studying population growth and density dependence, to take into account the initial conditions in which individuals have lived. Surprisingly, while many studies have looked at how acclimation to external conditions (light, temperature, pH) can affect density dependence, the impact of initial population density conditions on growth has never been studied. In this master's thesis, we studied how acclimation of a cyanobacterium of the genus *Synechococcus* to different population densities could impact organisms' traits and population growth, including the density dependence. We found that populations acclimated to higher densities showed higher mean trait values for all but one trait, but less variability. Growth modelling showed the emergence of a non-linear density dependence from a certain initial acclimation density. In addition, comparison of these functions showed that populations acclimated to higher densities had higher growth rates and lower density dependence. This study is the first to show how initial population density conditions can affect individual characteristics and population growth, including density dependence, and demonstrates that it is important to take a more general interest in all the historical conditions experienced by populations in order to better predict their dynamics.

Keywords : density acclimation, density-dependence, organisms' traits, population growth, *Synechococcus*.

Résumé

Dans un environnement en constant changement, il est nécessaire de comprendre comment différents facteurs peuvent impacter la croissance des populations, notamment sa dépendance à la densité, aussi appelée densité dépendance. Ces facteurs peuvent influencer directement les croissances des populations, induisant un taux de mortalité plus élevé par exemple, mais aussi indirectement, en changeant les caractéristiques des individus, telles que leur taille ou leur contenu en pigments, leur permettant de faire face aux conditions environnementales changeantes dans lesquelles ils se trouvent. Ce processus, aussi appelé acclimatation, peut fortement impacter la densité dépendance des populations. Il est donc nécessaire, lorsqu'on étudie la croissance des populations et la densité dépendance, de prendre en compte les conditions initiales dans lesquelles les individus se trouvent. De façon surprenante, Si beaucoup d'études se sont intéressées à comment une acclimatation à des conditions extérieures (lumière, température, pH) pouvait influencer cette densité dépendance, l'impact des conditions initiales de densité de populations sur leur croissance n'a jamais été étudié. Dans ce mémoire, nous avons étudié comment l'acclimatation d'une cyanobactérie du genre *Synechococcus* à différentes densités de populations pouvait impacter les traits des individus et la croissance des populations, notamment la densité dépendance. Les populations acclimatées à de plus hautes densités ont montré des valeurs moyennes de traits plus élevées pour tous les traits excepté un mais une variabilité moins importante. La modélisation de la croissance a montré l'émergence d'une densité dépendance non linéaire à partir d'une certaine densité initiale d'acclimatation. De plus, la comparaison de ces fonctions a montré que des populations acclimatées à de plus hautes densités présentaient des taux de croissances plus élevés et une densité dépendance plus faible. Cette étude est la première à mettre en avant l'impact des conditions initiales de densité de population sur les caractéristiques des individus et les croissances des populations, dont la densité dépendance, et démontre qu'il est important de s'intéresser de façon plus générale à l'ensemble des conditions historiques vécues par les populations afin de mieux prédire leurs dynamiques.

Contents

List of Figures

List of Tables

1 Introduction

1.1 Context

The current era in which we live is characterized by constantly changing environments. Some of these changes are threatening the conservation of species across the globe. At the population level, many events, sometimes induced by human activities, can lead to large reductions in the number of individuals in a population, with harmful consequences for its stability over time. When conditions allow, populations will grow back to their initial size before the disturbance. While growth is rapid at the start, it will slow down as the population approaches the size before the disturbance. Thus, this growth can be described by the following function :

$$\frac{dN}{dt} = N \cdot f(N) \tag{1}$$

where, $\frac{dN}{dt}$ is the population growth rate, N is the population size, representing the number of individuals in the population and f(N) is the function linking the population size and its growth. This dependence of a population's growth on its own size is known as density dependence. The density dependence comes from some constraints imposed by the increase of the population, like competition for resources (Levin and Chao, 1977). In addition, there is now a large body of literature showing that the conditions in which populations have lived will influence their density dependence (Nalley et al., 2018; Leroi et al., 1994; Xiong et al., 2000). This is due to the fact that organisms acclimate to these conditions, in particular by changing their characteristics, also known as traits (Clearwater et al., 1999; Muramatsu and Hihara, 2012). These adaptations, which can occur rapidly, enable individuals to thrive in their environments, subsequently influencing population growth (Layden et al., 2022). It is therefore necessary to take account of the population acclimation to these external variables in order to predict the density dependence more accurately. Surprisingly, while the effect of population acclimation to different variables on their growth is well-known, no study has investigated the impact of population acclimation to density on the density dependence. Nevertheless, some experiments indicated that organisms modified their traits in reaction to shifts in population density (Qiang et al., 1996; Ren et al., 2017). As we have seen that organisms' traits can affect their population growth, it is likely that acclimation to a population size has a direct effect on its density dependence.

1.2 Objective

The goal of this study is to investigate more accurately how organisms acclimate to population density and how this acclimation affects the density dependence of population growth. We used a cyanobacteria of the genus *Synechococcus*. Indeed, *Synechococcus* is widely distributed around the globe and has a major ecological role in all oceans (Flombaum et al., 2013; Wang et al., 2022). In addition, this cyanobacteria genus possesses complex light-harvesting structures known as phycobilisomes, composed of phycobiliproteins, themselves made up of an apoprotein covalently bound to a chromophore (Ting et al., 2002; Sui, 2021). As well as being efficient at capturing energy, this system features a variety of chromophores, enabling it to absorb a broader spectrum of light (Stadnichuk et al., 2015). Moreover, several studies have shown that the composition and functioning of this system can be strongly affected by various environmental conditions (Babu et al., 1991; Aráoz and Häder, 1997). The presence of this structure therefore allows us to investigate the effect of density on a wider variety of traits, making *Synechococcus* a relevant model for this study.

We acclimated populations to different densities and measured their mean trait values and the variability between individuals. Indeed, while mean values can provide initial insights into the adaptation of *Synechococcus* populations, exploring variability can also offer further information on the influence of density pressure on these populations. Once the populations had been acclimated, they were returned to new concentrations to measure their growth at these new densities. To the best of our knowledge,this two-step procedure has never been used before to measure density dependence. This experiment is therefore innovative in terms of both the research question and the methodology.

Our results indicated a significant effect of density acclimation on organisms' trait values and on population growth. Density increase led to higher mean trait values but lower trait variability. The density acclimation also led to significant changes in density dependence modeling, with the emergence of non-linear effects. In addition, populations acclimated to higher densities exhibited higher overall growth rates and weaker density dependence.

2 Material and methods

2.1 Experiment

2.1.1 Study system

We investigated the influence of density acclimation on individual trait values and population growth in the clonal strain *Synechococcus* sp. RS 9909, from the Roscoff Culture Collection. We conducted two experiments, each divided in two phases. The first phase, called the acclimation phase, consisted of acclimating cultures of bacteria to different densities (Supplements, Fig. S3). The method for producing acclimated cell culture differed between the two experiments (see procedure). The second phase, which we called space-for–time, was by contrast, carried out in the same way in both experiments. We applied several dilutions on the acclimated cultures to obtain new cultures at different densities (Supplements, Fig. S4). We then tracked the density changes for two days to calculate the growth rate at these new densities. The entire protocol is illustrated by Figure1. In the rest of the paper, the term "treatment" will refer to the different densities reached by cultures at the end of the acclimation phase.

2.1.2 Experiment setup

Throughout the duration of the experiment, cultures grew in white light (LED bar SKY 6500K) in a 12:12 dark/light cycle at 22°C and were mixed 150 RPM with a VWR mini shaker. The light intensity was adjusted and higher in the second method based on Roscoff station's recommendations (Supplements, Fig. S1 and Supplements, Fig. S2). These growing conditions were identical to those of stock cultures. The sampling sessions were done in a sterile hood. For the first phase, our microcosms consisted of two 6-well plates (Costar®) per treatment, filled with 4 mL of PCRS11 medium and 2 mL of cultures, inoculated at a concentration of 25 000 cells μL^{-1}. The recipe for the medium can be found in Rippka et al. (2000) and on Roscoff station website. Before inoculation, cultures were filtrated to avoid the presence of clumps. In the second phase, cultures were inoculated in new 6-well plates, with 3 wells for each new dilution.

2.1.3 Experimental procedure

The experiments were divided into two phases. In the first phase, the method of density acclimation differed between the two experiments that were carried out. In the first experiment, the acclimation phase consisted of letting our three populations reach densities of 50 000, 90 000 and 130 000 cells

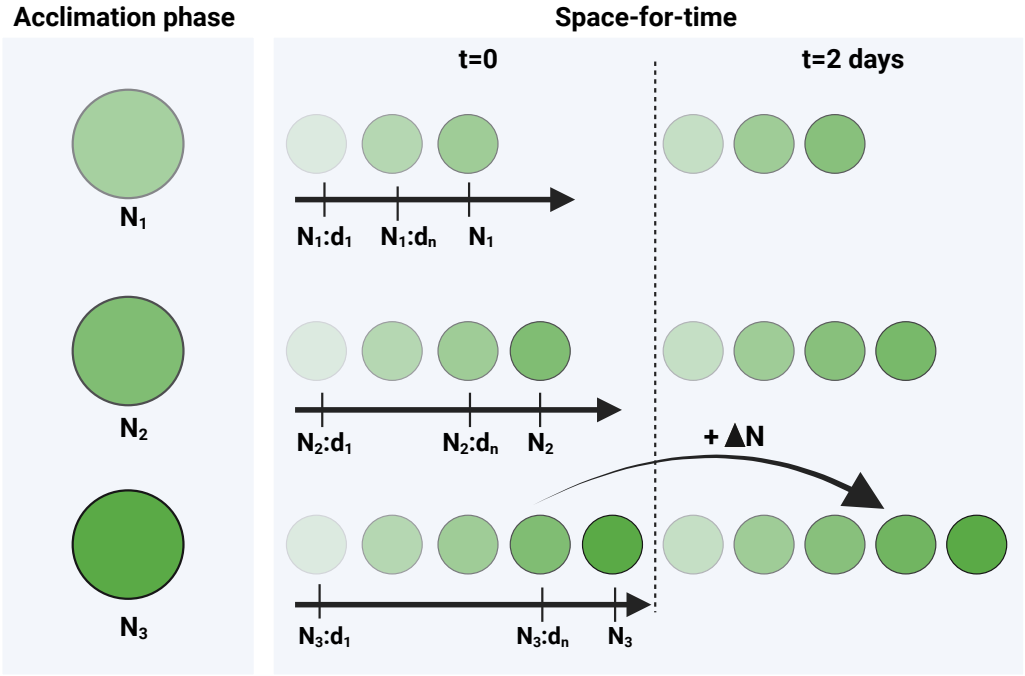

Figure 1: Schematic illustration of the two-phase experiment. During the acclimation phase, the initial cultures reached different population densities (Method 1 : $N_1 = 50\ 000$, $N_2 = 90\ 000$ and $N_3 = 130\ 000$ cells μL^{-1} ; Method 2 : $N_1 = 80\ 000$, $N_2 = 130\ 000$ and $N_3 = 170\ 000$ cells μL^{-1}). During the second phase, we performed several dilutions to obtain new densities. In method 1, the new densities obtained were 10 000, 20 000, 35 000, 50 000, 90 000 (when possible) and 130 000 (when possible) cells μL^{-1}. In method 2, the new densities obtained were 15 000, 30 000, 50 000, 70 000, 100 000 (when possible) and 150 000 (when possible) cells μL^{-1}. We then measured population densities and organisms traits for two days. This procedure is called space-for-time. The opacity of the green indicates population density.

μL^{-1}. As soon as they reached these densities, the cultures were diluted for two days to stabilize them at around these concentrations. The second method consisted of applying a respective daily dilution rate on each culture until they reached their carrying capacity. Every day, we removed 1/5 or 1/3 of each well, meaning 1.2 mL or 2 mL, and replaced by the same volume of fresh medium. A control population did not undergo any dilution. The cultures achieved final concentrations of 80 000, 130 000 and 170 000 cells μL^{-1}. In both experiments, every acclimated culture had 12 replicates.

For the space-for-time, methods were the same for both experiments. Once the acclimating cultures reached their carrying capacity, we mixed all replicates from a same culture in a sterile 100 mL Erlenmeyer, and measured the concentration of these suspensions through flow cytometry. Based on these new cultures, we carried out several dilutions to obtain new densities of 10 000, 20

000, 35 000, 50 000, 90 000 (when possible) and 130 000 (when possible) cells μL^{-1} for the first experiment. In the second experiment, we diluted the cultures to obtain new densities of 15 000, 30 000, 50 000, 70 000, 100 000 (when possible) and 150 000 (when possible) cells μL^{-1}. Each new dilution was represented by three replicates. We measured the population densities every day for two days.

2.1.4 Data acquisition

In both phases, population densities and individual traits were monitored every day through flow cytometry (Guava easyCyte 12HT) (Adan et al., 2016). Before sampling, 57 μL of distilled water was added to counteract evaporation. After that, for each treatment, 200 μL of culture were sampled from every well and transferred to a 96-well plate. In first phase, the 200 μL sampled were replaced with 200 μL of fresh medium. In second phase, we did not add fresh medium to avoid influencing growth rate values through dilution. The 96-well plate was then inserted into the flow cytometer to measure the traits of the organisms and the density of populations. The traits measured were cell size (FSC) and complexity (SSC), chlorophyll-a (RED.B), phycoeryhtrin (YEL.B) and phycocyanin contents (RED.R). The exact flow cytometry procedure can be found in the appendix A.2.

2.2 Analyses

The analyses carried out differed between the two phases of the experiment. The aim of the acclimation phase was to figure out the effect of density acclimation on organisms' trait values. The densities of populations as well as organisms' traits were tracked on a daily basis. Moreover, final density and trait values were compared between treatments. For density, we conducted a linear model of the final density achieved according to the treatment. If homoscedasticity was not respected, then a Kruskal-Wallis test was performed to detect any global differences between treatments. Furthermore, we also compared the final densities between plates. Sometimes we had to we remove a plate of a treatment to avoid problems of heteroscedasticity. Although this method does not permit us to draw conclusions about differences between treatments, it does allow to observe differences between plates and to observe potential causes of non-compliance with the conditions of use of linear models. The same methodology was used for the mean trait values and the variability between individuals within the same population. For trait variability, we first extracted the per-cell data of each replicate. Based on these data, we calculated the standard

deviation of each well. Thus for a treatment, we had 12 values of standard deviation per day. In the first experiment, we also conducted some contrast analyses using the Bonferonni correction to compare final standard deviation of traits between plates, as there was high variation in one of the acclimated cultures. As a complementary analysis, a PCA was executed to better visualize the differences between the treatment at the start and at the end of the acclimation phase.

The aim of the second phase was to figure out if density acclimation had an effect on population growth, especially their density dependence. Acclimated populations were diluted to new densities in order to calculate the growth rates at these new densities. These growth rates were calculated with the equation $\gamma_t = \Delta^{-1} \log\left(\frac{N_{t+\Delta}}{N_t}\right)$ where Δ was the time between sampling sessions, and N_t the population density at the start of the second phase. Here, the Δ was equal to two days. For each treatment, we fitted the growth data to polynomial models with a maximum degree of four of γ_t against N_t :

$$\gamma = \beta_0 + \beta_1 N + \beta_2 N^2 + \beta_3 N^3 + \beta_4 N^4 \tag{2}$$

Where γ is the per-capita growth rate, N is the population density and β_0, β_1, β_2 , β_3 and β_4 are the regression coefficients. We compared the most complex model with models where β_2 , β_3 and β_4 coefficients were equal to zero and chose the best through the AIC criterion. When two treatments were fitted to models with the same degree, we added the treatment variable and its interaction with the density variable. Finally, we calculated the derivatives of the growth functions in order to better describe the density dependence between the treatments along the density gradient.

3 Results

3.1 Changes in density

In both methods, the populations, starting from similar concentrations, reached different final concentrations (Supplements, Fig. S5). In method 1, we detected an overall effect of the treatment on the final densities achieved (Kruskal-Wallis test, $\chi^2 = 24.889$, df = 2, p = 3.94e-06). The large variation in densities achieved in the highest density treatment can be attributed to a significant difference in final densities between the treatment plates and to a wide variation within one plate of the treatment (Supplements, Fig. S6). In method 2, the densities of the treatments were also significantly different (Figure 2). The maximal densities achieved were higher than in the first method.

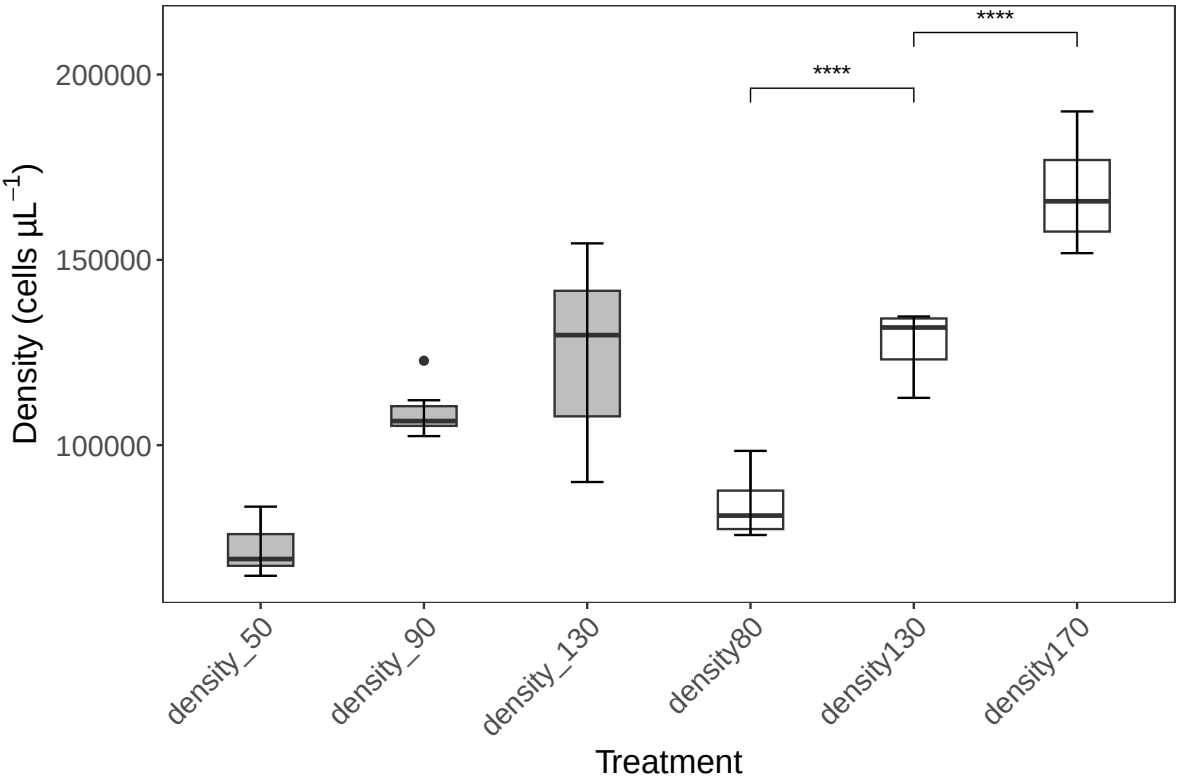

Figure 2: Final acclimation densities. Grey bars refer to the method with dilutions when population reached their equilibrium (n = 36) and white bars refer to the method with a daily factor of dilution (n = 36). The figure shows median population densities (lines), 25% to 75% quartiles (boxes) and ranges (whiskers). Black dots are shown if extreme values are more than 1.5 times the interquartile range of the box. * $p < 0.01$, ** $p < 0.001$, *** $p < 0.0001$.

3.2 Density acclimation effect on trait values

3.2.1 Mean trait values

In both methods, the treatments exhibited different final values for almost every trait (Figure 3, Supplements, Fig. S7). Both FSC and SSC were greater for higher density treatments (Figure 3AB and Supplements, Table S1). This indicated that cells were bigger and more complex at higher densities. Treatments of equivalent density but from different methods (e.g. density_130 from method1 and density 130 from method2) showed similar values for FSC. However, SSC values were overall higher in the second method than in the first one, even for similar densities.

For pigment contents, responses to density conditions varied according to the pigment. Treatments showed significant differences in RED.B values (Figure 3C, Supplements, Table S1). In both methods, these trait values were higher in denser populations, suggesting that cell contained more chlorophyll-a in response to density increase. YEL.B showed similar results, though differences were

not always significant between the treatments (Figure 3D, Supplements, Table S1). As for FSC, pigment contents did not clearly differ between similar density treatments from the two methods, or at least not in a consistent way.

No clear pattern was observed in final RED.R contents (Figure 3E). However, substantial variation was found in some treatments (Supplements, Fig. S8). For the method 1, this substantial variation in treatments was also found in the corresponding plates. The variation in method 2, more specifically in the highest density treatment, was rather due to large differences between the plates of this treatment.

3.2.2 Standard deviation of traits

The standard deviation of each trait clearly expressed a decrease when density increased (Supplements, Fig. S9). When looking at the final standard deviation of each trait, results also showed clear differences of variability between treatments for both methods (Figure 4). For the first method, important variation in the density_130 prevented the performance of ANOVA tests. However, based on graphic observations, it is clear that higher density treatments exhibited weaker variation in each trait. To support these observations, we performed contrast analyses to compare traits standard deviation of each plate, removing plate E because of large variation (Supplements, Table S2). Two plates from a same treatment never showed any difference in standard deviation of trait. However, two plates of two different treatments always exhibited a final different standard deviation for each trait.

The patterns observed in the first method were confirmed by the results of the second experiment. Every trait had weaker variation in higher density treatments compared to lower density treatments (Figure 4). Differences between density80 and density130 treatments were always significant, as well as between density80 and density170 treatments. However, differences in standard deviation between density130 and density170 treatments appeared to be significant only for SSC, RED.R and RED.B.

Based on the results of the acclimation phase, we can conclude that density acclimation impacts both the mean values and the variability of *Synechococcus*' traits, in a quite predictable way (Figure 5). PCA analysis supported these results by showing evident distinctions between treatments and also differences within treatments between the start and the end of the acclimation phase (Supplements, Fig. S10). In both methods, a substantial part of the variation in our data

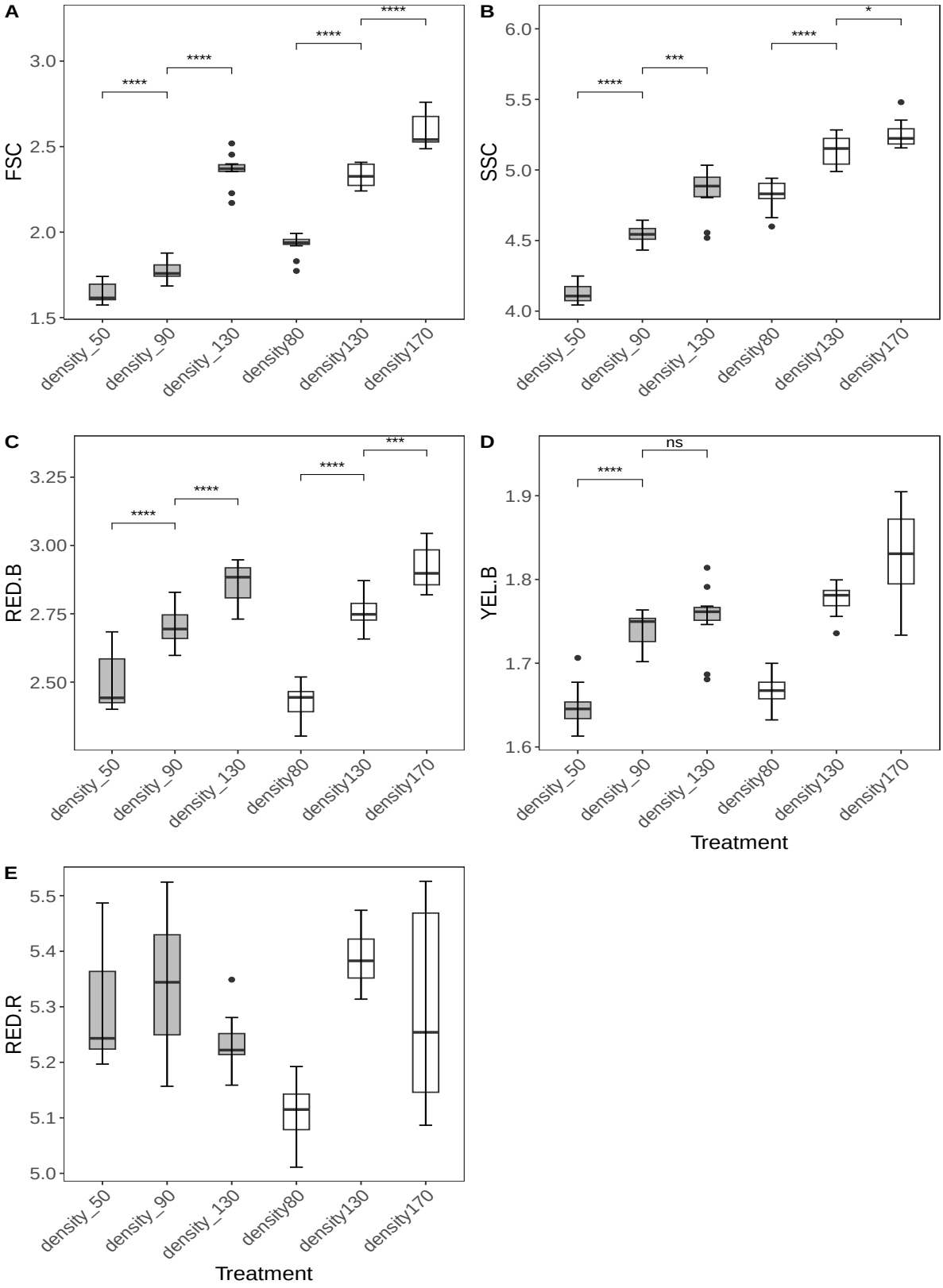

Figure 3: Final mean trait values. Grey bars refer to the method with dilutions when population reached their equilibrium (n = 36 for each trait) and white bars refer to the method with a daily factor of dilution (n = 36 for each trait). The figure shows median trait values (lines), 25% to 75% quartiles (boxes) and ranges (whiskers). Black dots are shown if extreme values are more than 1.5 times the interquartile range of the box. * $p < 0.01$, ** $p < 0.001$, *** $p < 0.0001$.

was explained by the combination of the two axes. The next question to explore is whether this change in *Synechococcus*'traits has an influence on the density-dependence of population growth.

3.3 Density acclimation effect on population growth

Figure 6 shows the density-dependence of *Synechococcus*' growth for both methods. Density acclimation had a larger effect than expected on the density dependence function, as this caused a switch from linear to polynomial models for highest density acclimated populations. In addition, results also indicated that high density acclimation led to a higher intrinsic growth rate and a weaker density dependence.

In the first method, the degrees of the polynomial models differed between the density treatments, indicating a significant effect of density acclimation on the density dependence of growth (Figure 6A and Supplements, Table S3). While the lowest density treatment was better fitted to a linear regression, the two others were fitted to polynomial regressions of a degree three. When comparing only these two last treatments, the highest density treatment exhibited a higher intrinsic growth rate and a global faster growth. A common characteristic of these two treatments is that their populations achieved a growth optimum at a density of around 35,000 cells/μL^{-1} . After this density, growth started to decrease when density increased. The derivatives of the functions indicated that populations acclimated to higher densities exhibited weaker density dependence (Supplements, Fig. S11). Indeed, the derivatives of polynomial functions were always less negative than that of the linear function. In addition, when comparing the derivatives of the polynomial functions, the highest density treatment showed a less negative derivative up to a population density of 70,000 cells μL^{-1}.

In the second method, the degree of the models also differed between the density treatments. Here, only the highest density treatment exhibited a non-linear regression. This function exhibited two optimum values, a first one around 35 000 cells/μL^{-1} and a second one around 135 000 cells/μL^{-1}. When we compared only the two models showing linear regression, the low density acclimated treatment had a lower y-intercept and a steeper slope, indicating a lower intrinsic growth rate and a stronger density dependence (Supplements, Table S4).

While the density_130 treatment from the method 1 showed a polynomial regression, the density 130 treatment from method 2 was better fitted to a linear model. It therefore seems that the threshold value at which density dependence became non-linear was higher in method 2 than in method 1.

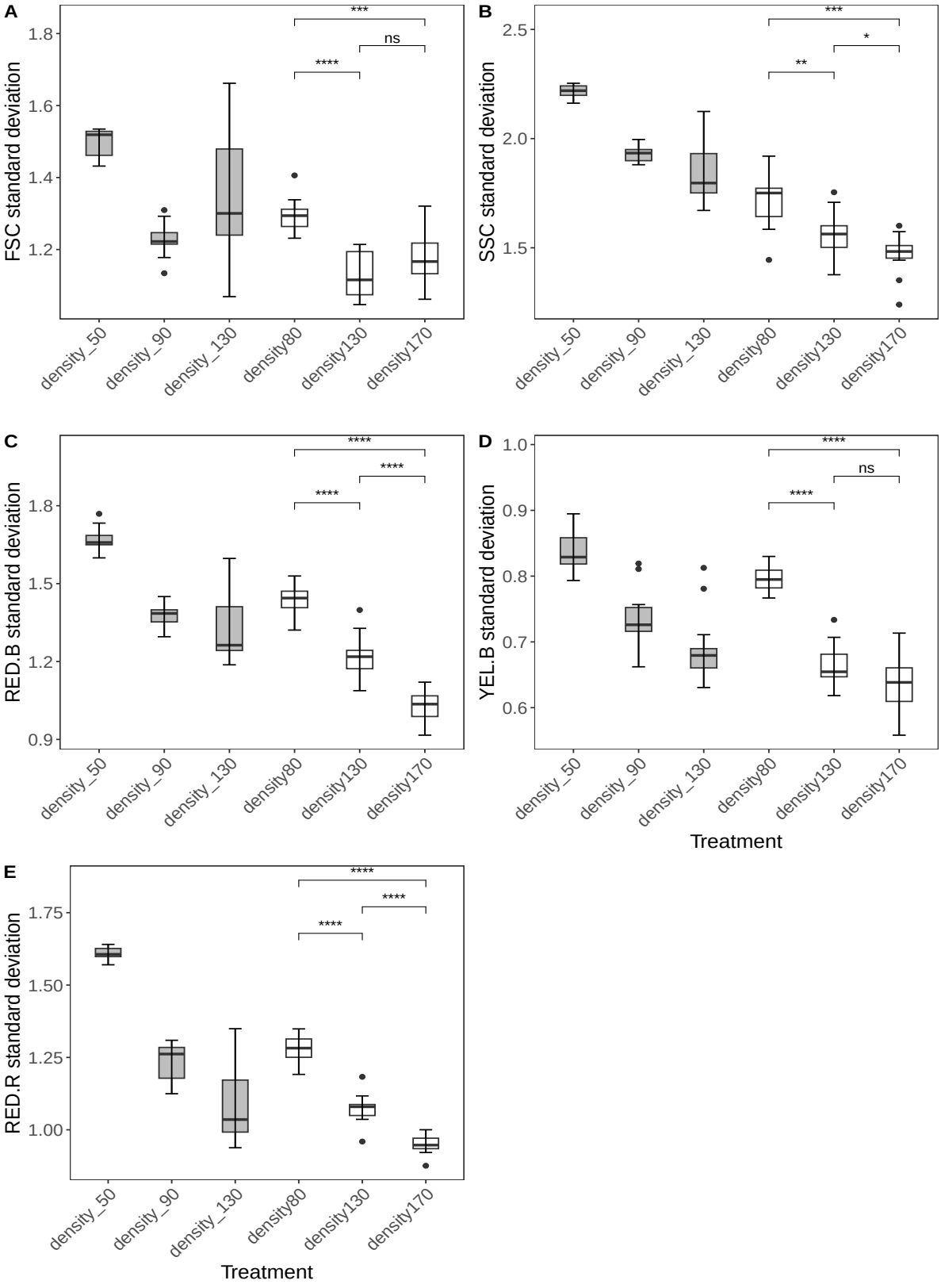

Figure 4: Final standard deviations of traits. Grey bars refer to the method with dilutions when population reached their equilibrium (n = 36 for each trait) and white bars refer to the method with a daily factor of dilution (n = 36 for each trait). The figure shows median standard deviation values (lines), 25% to 75% quartiles (boxes) and ranges (whiskers). Black dots are shown if extreme values are more than 1.5 times the interquartile range of the box. * $p < 0.01$, ** $p < 0.001$, *** $p < 0.0001$.

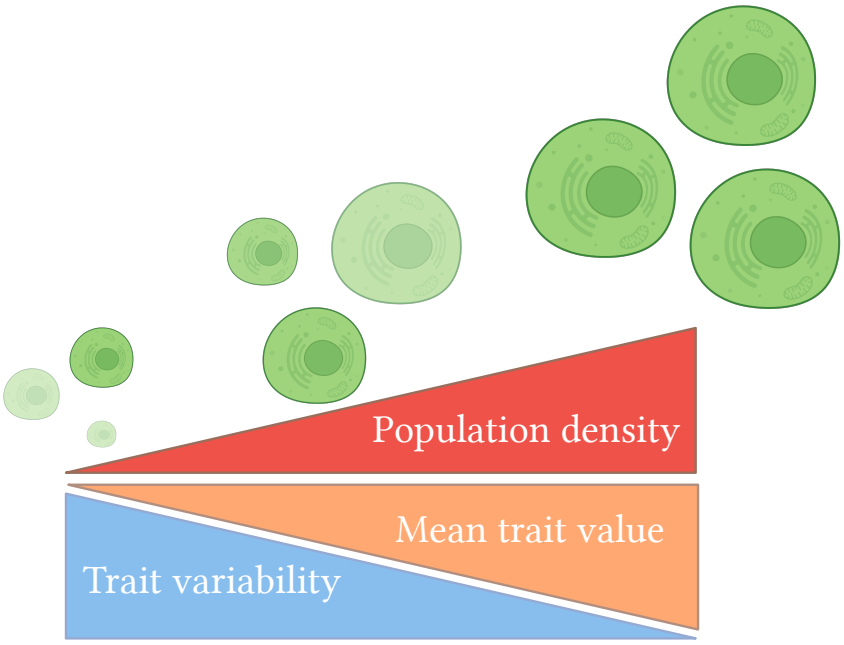

Figure 5: Acclimation of *Synechococcus* populations to density. Cells become bigger and more pigmented when density increases, but the variability within the population decreases.

Overall, results undeniably indicated an effect of density acclimation on *Synechococcus*' traits and growth. Populations acclimated to higher densities showed higher mean trait values, except for phycocyanin, but less variability (Figure 5). Modeling the density-dependence suggested faster growth in high-density acclimated populations and weaker density dependence. In addition, mathematical relationships between density and growth were sometimes completely different between the treatments, with non-linear relationships emerging. The effect of density acclimation on the density dependence function was thus more complex than expected.

4 Discussion

4.1 Evaluation of the experimental procedure

A first point of discussion regarding this experiment concerns the experimental protocol used to study the effect of density acclimation on organisms' traits and population growth. For the first phase, we employed two methods of acclimation. After testing them, we were able to determine the advantages and disadvantages of each method. The first method, which consisted of allowing cultures to grow before stabilising them, enabled us to investigate the effect of acclimation to density itself on cyanobacteria populations. However, this method lacked precision in achieving the

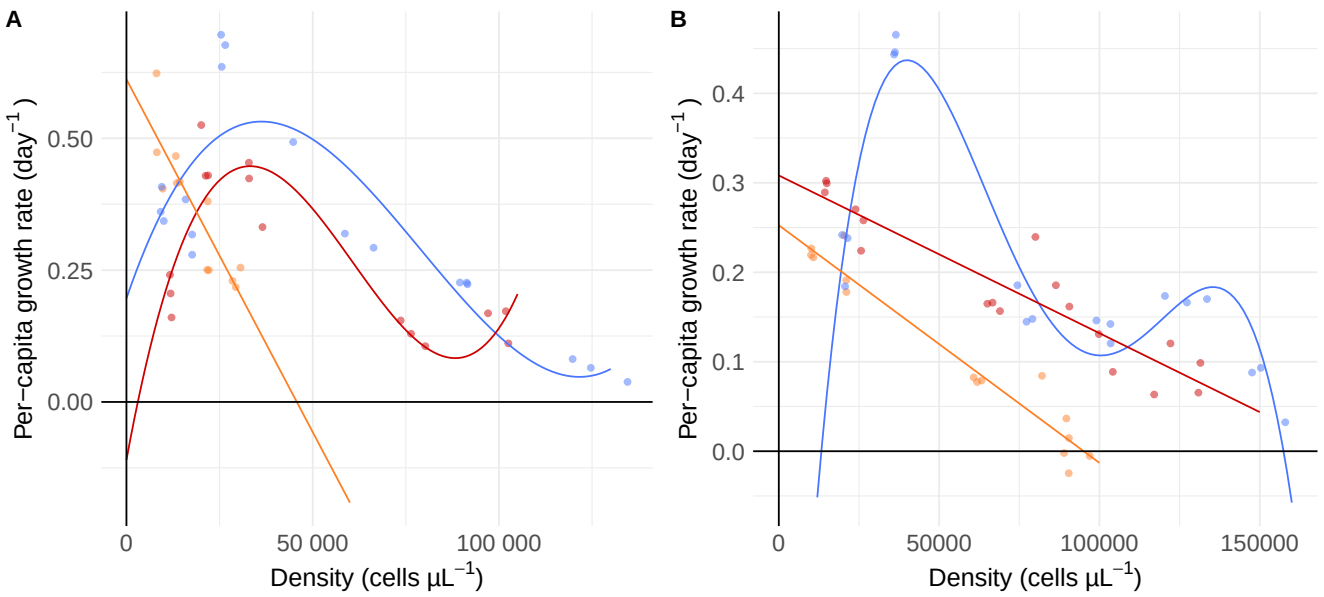

Figure 6: Density dependence of *Synechococcus*' growth. Dots correspond to experimentally calculated growth rates and curves correspond to the estimated growth models. A : method of acclimation with dilutions when population reached their equilibrium. Orange : density_50 (n = 12), red : density_90 (n = 15), blue : density_130 treatment (n = 18). B : method of acclimation with a daily factor of dilution. Orange : density80 (n = 15), red : density130 (n = 18), blue : density170 treatment (n = 18).

targeted population densities. Indeed, the population acclimated to the highest density showed significant variation in the final densities reached among replicates. One potential reason for this imprecision is that, in order to maintain populations at a similar density between replicates, each underwent a more or less substantial dilution. It is possible that excessive dilution caused disturbances in some populations, impacting their stability. In addition to this imprecision, the other two treatments reached higher densities than expected. This may be explained by the rapid growth of the strain, making its regulation complicated. It would have been interesting to monitor density changes at shorter time intervals to better regulate their densities at the end of the acclimation phase. In the second method, where we applied a dilution to the cultures every day, the control of density was more continuous and regular. We were therefore able to bring the populations more precisely into the targeted densities. However, as dilution rates differed between populations, the cultures here did not differ only by the final density achieved, but also by the way they achieved this density. Thus it was impossible to separate the effect of density and the method of acclimation on the traits of organisms and growth of the populations. Despite the downsides of each method, one strong point of the study is that we were able to observe the same patterns of

trait values between treatments in both experiments, enabling us to generalize the effect of density acclimation on individual traits. For the second phase, we used the space-for-time method to measure growth rates at different densities, while removing the time effect. In previous experiments, density dependence was measured over the entire growth curve of the same population (Krichen et al., 2018). However, in this kind of procedure, density is correlated with time. As we have seen here, traits can change quite rapidly over time. These changes in traits can therefore have an effect on the density dependence of populations. In our case, by diluting a density acclimated population to new densities and measuring the growth rate over a relatively short time, we were able to limit trait change, thereby isolating the effect of density on population growth. This procedure therefore seems appropriate for studying the specific effect of density on population growth, removing the effect of other variables such as time.

4.2 Density acclimation effect on trait values

Our experiments demonstrated that density acclimation has a large influence on *Synechococcus*' traits. Higher density led to higher mean values and lower variability for all the traits studied, except the phycocyanin. For the cell size, observing a positive effect of density on cell size was quite unexpected, according to the literature. Most of studies investigating the link between cell size and population density found a negative effect (Agusti et al., 1987; Ward et al., 2012). This usually comes from constraints to the increase in size, like internal and external diffusion, linked to resources uptake and distribution, but also intracellular light and CO_2 levels that decline from the cell membrane to the center (Wirtz, 2011). Therefore, as an increasing density leads to a decrease in resources, we would have expected a decrease in cell size. However, this constraint in cell size can be overcome by an increase in cell internal complexity (Okie, 2013). This strategy would allow organisms to maximize the uptake and diffusion of resources. The increase of SSC, which can be used as a proxy of the cell complexity, could suggest that *Synechococcus* is able to overpass these size constraints in dense environments through a higher cell complexity. If this is the case, then we can hypothesize that this cell size increase is a competitive strategy to maximize light capture, light being more limited in more densely populated environments. Bigger organisms will be more exposed to light and less in the shadow of other individuals. This greater availability of light would enable them to maximize photosynthetic activity, in order to produce resources such as carbohydrates. This strategy is also found in complex multicellular organisms, such as seagrasses, that exhibit wider leaves in deep waters to maximize light capture efficiency (Dalla Via et al., 1998).

This hypothesis of increasing cell size to maximize light capture is also supported by the changes in pigment contents. Both chlorophyll-a and phycoerythrin levels were increasing with density. These patterns are usually found in other photosynthetic organisms in limited light conditions. Multiple studies demonstrated that chlorophyll-a was increasing when light availability was reduced and inversely, whether in plankton, macrophytes or plants (Krause-Jensen and Sand-Jensen, 1998; Minotta and Pinzauti, 1996). This pattern was also demonstrated for phycoerythrin (Six et al., 2004; Xie et al., 2021). If this pigment content trend was observed for chlorophyll-a and phycoerythrin, we have not been able to discern any clear pattern of the phycocyanin pigment content. An explanation could be the high variability of this pigment content in our cultures. Despite no clear trend of phycocyanin content, some examples in the literature showed that the phycocyanin content was increasing in light-limited conditions (Hoi et al., 2021).

Thus, our experiment is one of the first showing the clear response of *Synechococcus*' cell morphology and pigment contents to population density increase. More specifically, it appears that the cyanobacteria is responding to density increase as it responds to light limitation, by maximizing the cell size and complexity, as well as the pigment contents. This finding opens the door to many new questions. First, as the effect of density and light seem to be similar on trait values, we should investigate the effect of density on these traits under different light intensity conditions, to better differentiate the effect of these two variables. Second, if pigments seem to increase with population density, it would be interesting to better study the relative contents between them. Indeed, if some experiments showed that the ratio phycocyanin/chlorophyll-a in *Spirulina platensis* was unaffected by the light intensity, other experiment found out the opposite in *Microcystis aeruginosa* (Raps et al., 1983; Kumar et al., 2011). In our case, such comparisons were limited by the use of proxies rather than direct measurement of traits, as we do not know the exact function linking the accurate trait value and the proxy. Therefore, complementary methods of trait measurements should be used to better evaluate the density dependence of absolute and relative pigment contents.

While the experiment has demonstrated an effect of density on trait values at the individual level, we have little information about how the molecular mechanisms were affected. Previous tests in mammalian cells showed that density changes altered a set of genes involved in metabolism and growth, leading to confounding experimental results (Trajkovic et al., 2019). This prompts us to better characterize the molecular pathways involved in cell morphology and photosynthetic activity, as well as defining the impact of density on these pathways.

For cell size, knowledge on the genetic control of this trait is quite recent and the entire pathway is not yet fully understood, the effect of density on it even less. Recent studies showed that the cell size in some cyanobacteria is controlled by a two-component signaling system using the cyclic-di-GMP as a messenger (Xie et al., 2021; Zeng et al., 2023). This messenger is often used in other bacteria as a signal molecule to detect population densities by quorum sensing (Ramírez-Mata et al., 2014). Quorum sensing is therefore an option to explain how *Synechococcus* is able to detect any changes in population density in its environment. However, as *Synechococcus* is a photosynthetic organism, it is quite possible that the changes in population densities are indirectly detected through changes in light intensity or wavelength thanks to bacteriophytochromes. The presence of such light sensors has already been reported in some cyanobacteria species (Lamparter et al., 1997). The connection between the perception of changes in light in plants and their subsequent responses, including alterations in growth, is now understood to be mediated by the signaling pathway of phytochromes (Ding et al., 2021). We have thus identified two potential mechanisms for controlling cell size through population density. Based on our experiments, it is impossible to identify which one is actually used by *Synechococcus*. Further studies should explore the potential presence of an extracellular signaling molecule that would validate the quorum sensing hypothesis and indicate that cell size is directly mediated by the population density or the presence of some light-sensors like bacteriophytochromes, indicating that light is the main factor regulating cell size.

For chlorophyll-a pigment, a recent study showed that plants acclimated to low-light conditions upregulated their electron transport capacity, by increasing their chlorophyll and their light-harvesting protein contents, but also their level of cytochrome b6f and ATP synthases (Ermakova et al., 2021). In addition, the PSII/PSI ratio was enhanced in low light conditions, suggesting an investment in light capture. Another study showed that photosynthesis genes in *Arabidopsis thaliana* where upregulated in response to density stress (Geisler et al., 2012). Our results are therefore in line with the literature and indicate that *Synechococcus* responds to an increase in density in the same way as it responds to a decrease in light. Future experiments should nevertheless focus on the specific evolution of molecular components linked to the light and dark phases of photosynthesis, while linking this with measurements of photosynthetic activities, such as oxygen production. For the phycobiliproteins, some experiments suggested that the regulation of phycoerythrin cellular levels in response to light changes also involves some complex posttranscriptional processes (Anderson and Grossman, 1990).

While the mean trait values were increasing with density, the variability showed the opposite trend. This variability reduction could highlight the intraspecific competition due to a higher density pressure on the individuals. As a higher density of population usually induces a higher competition for resources, organisms in denser populations should show the optimal trait values and will outcompete those with sub-optimal values, leading to a reduce in variability between individuals. However, the phycoyanin, which also showed a reduction in variability between individuals, exhibited no discernible trend in the shift of its mean value. This reduction in variability is therefore not sufficient to infer that there is selection pressure on trait values. In addition, the exact mechanisms underlying the trait changes are not really known. In this experiment, since the cultures were derived from a clonal strain, the changes in traits were probably due to phenotypic plasticity (Gibert et al., 2022; Koch et al., 2017). However, in populations with genetic variation, it is possible for traits to change through natural selection. It would therefore be interesting to quantify the role of each of these mechanisms in density acclimation in natural populations.

While the intraspecific competition led to higher mean trait values and a lower variability, it would be interesting to compare how density can influence the traits of two or more interacting strains. Indeed, a first possibility would be that strains show the same responses to density changes, which would suggest a competition between the two species, potentially leading to the exclusion of one of them. An alternative option would be that strains tried to reduce the competition by changing their traits in order to optimize resources sharing. This second option has already been described and used to explain how a wide range of plankton species can live in a quite homogeneous environment (Spaak and De Laender, 2021; Huisman et al., 2001; Stomp et al., 2004). This type of experiment would enable us to learn more about the effects of density in individuals of the same or different species.

4.3 Density acclimation effect on population growth

The second main objective of the study was to investigate the effect of acclimation to density on *Synechococcus*' population growth. In the first experiment, the density acclimation had a large effect on the density dependence modeling. For the two highest density treatments, the density acclimation resulted to the emergence of inverse density dependence, also known as the Allee effect (Courchamp et al., 1999). This was quite unexpected, as this effect has been rarely observed in some microorganisms with asexual reproduction (Ohkawa et al., 2020).The presence of the Allee effect for the higher density treatments but not for the lower one could indicate that acclimation to

high population density led to a non-adaptation to less dense environments. This was supported in part by the better performance of low-density acclimated populations in lower density conditions than high-density acclimated populations. When comparing only the populations showing the Allee effect, the highest-density acclimated population showed faster growth than the other one, with a higher intrinsic growth rate and a weaker density dependence, at least up to a certain population size. In the second experimental approach, we observed similar trends to those observed in the first method, indicating the emergence of the Allee effect and a more pronounced density dependence for populations acclimated to lower densities. However, a noteworthy distinction was the delayed onset of non-linear density dependence in the second method compared to the first one. While the difference in the acclimation methods might contribute to this disparity, it appears insufficient to account for the observed difference alone. Another variable that underwent a change between these two experiments was the light conditions. Specifically, bacterial populations in the second experiment were exposed to a higher light intensity compared to those in the first experiment. If we consider that the impact of density acclimation is, at least in part, influenced by the adaptation of individuals to light availability, it is reasonable to infer that the threshold value for non-linear density dependence is, to some extent, determined by light conditions. This may elucidate why non-linear density dependence was observed at higher acclimation densities in the second method compared to the first. Although this result should be treated with caution, as factors other than light may also have played a role, it shows that the environment itself can modify the effect of density acclimation on density dependence. It now seems important to better characterize this effect of the environment with the variation of several resources potentially limiting growth, such as the quantity and quality of light, but also the quantity of nutrients, or temperature for example.

Another important aspect to study here is the relationship between organisms' traits and population density dependence. In our experiment, the emergence of the Allee effect may suggest that individuals acclimated to high densities had traits that were not adapted to lower densities. However, when considering only treatments fitted to models with the same degree, we can observe that populations acclimated to higher densities had higher growth rates. These populations were composed of individuals that exhibited the highest trait values. Therefore, we can say that populations with higher trait values were also those showing the fastest growth. This parallel can be supported by the Metabolic Scaling Theory, that states that the pace of organism processes, such as the metabolic rate or even the population growth rate, are an exponential function of the

individuals' size with the following equation:

$$Y = Y_0 M^b \tag{3}$$

where Y is the population growth rate in our case, M is the body mass, and b is the scaling exponent (Brown et al., 2004; DeLong et al., 2010). The main information to be drawn from this theory is that the population growth rate is positively related to the size of the individuals making up the population. What is interesting about our experiment is that it both confirms and contradicts this theory, even though this relationship was not directly studied. Indeed, we observed that populations acclimated to higher densities had higher trait values, including the cell size, and higher growth rates. However, this relationship was only correct at certain densities, as we have found that from a certain density acclimation threshold, individuals were less adapted to lower densities and therefore show lower growth rates than predicated by the Metbabolic Scaling Theory. It is therefore likely that density acclimation impacts this relationship between individual traits and population growth. Other studies revealed that the size-scaling of growth of phytoplankton populations changed also in different light and nutrient availability conditions (Mei et al., 2009). Based on the literature and our results, we can see that the link between individual characteristics and population growth is intimately close but also modulated by several factors, whether population densities or environmental variables. Future studies should attempt to quantify the effects of each ecological level on the others in order to better understand how acclimation to a variable, such as density, can affect individual and population dynamics.

5 Conclusion

While many studies investigated the effect of acclimation to different environmental factors on organisms' traits and population growth, this experiment is the first one to describe the impact of density acclimation on these features. During the acclimation phase, organisms exhibited an increase in nearly all their trait values in response to higher density. Simultaneously, there was a reduction in inter-individual variability. These findings were strengthened by the consistency across both experiments.

For the density dependence of population growth, both experiments showed that density acclimation has a significant effect on density dependence. Indeed, organisms that were acclimated to higher densities showed higher growth rates and a weaker density dependence. In addition, the emergence of non-linear density dependence indicated an even greater and more complex effect of density acclimation than expected. The later appearance of a non-linear relationship in the second experiment may suggest that light influences the effect of density acclimation on density dependence, which would illustrate the complexity of the interactions between individual traits, population dynamics and the environment surrounding these populations. However, since our experiments differed in more than one variable, it is difficult to draw strong conclusions about the respective impact of experimental conditions, such as light intensity or the method of acclimation.

Yet, this study opens up new avenues of research to better understand how populations' characteristics, such as density, can modify their entire dynamics. In addition to the improvements already suggested in the paper, we believe that this type of study can be repeated on new strains presenting other trait and growth values in order to see the potential generalization of the effect of density acclimation. Changes in the environment, such as temperature, light or even the presence of competing species, can also help us better understand the interactions between density-dependent and non-density-dependent variables, and their effects on individual traits and population dynamics.

As a conclusion, this study showed that the initial density conditions of populations can have a strong impact on their growth, and that they must be taken into account to better predict population dynamics.

6 References

References

A. Adan, G. Alizada, Y. Kiraz, Y. Baran, and A. Nalbant. Flow cytometry: Basic principles and applications. *Critical Reviews in Biotechnology*, page 1–14, 2016. doi: 10.3109/07388551.2015.1128876.

S. Agusti, C. M. Duarte, and J. Kalff. Algal cell size and the maximum density and biomass of phytoplankton1. *Limnology and Oceanography*, 32(4):983–986, 1987. doi: 10.4319/lo.1987.32.4.0983.

L. K. Anderson and A. R. Grossman. Structure and light-regulated expression of phycoerythrin genes in wild-type and phycobilisome assembly mutants of synechocystis sp. strain pcc 6701. *Journal of Bacteriology*, 172(3):1297–1305, 1990. doi: 10.1128/jb.172.3.1297-1305.1990.

R. Aráoz and D.-P. Häder. Ultraviolet radiation induces both degradation and synthesis of phycobilisomes in nostoc sp.: a spectroscopic and biochemical approach. *FEMS Microbiology Ecology*, 23(4):301–313, 1997. doi: 10.1111/j.1574-6941.1997.tb00411.x.

T. S. Babu, A. Kumar, and A. K. Varma. Effect of light quality on phycobilisome components of the cyanobacterium spirulina platensis. *Plant Physiology*, 95(2):492–497, February 1991. doi: 10.1104/pp.95.2.492.

J. H. Brown, J. F. Gillooly, A. P. Allen, V. M. Savage, and G. B. West. Toward a metabolic theory of ecology. *Ecology*, 85(7):1771–1789, 2004. doi: 10.1890/03-9000.

M. Clearwater, R. Susilawaty, R. Effendi, et al. Rapid photosynthetic acclimation of *Shorea johorensis* seedlings after logging disturbance in central kalimantan. *Oecologia*, 121:478–488, 1999. doi: 10.1007/s004420050954.

F. Courchamp, T. Clutton-Brock, and B. Grenfell. Inverse density dependence and the allee effect. *Trends in Ecology & Evolution*, 14(10):405–410, 1999. doi: 10.1016/S0169-5347(99)01683-3.

J. Dalla Via, C. Sturmbauer, G. Schönweger, E. Sötz, S. Mathekowitsch, M. Stifter, and R. Rieger. Light gradients and meadow structure in posidonia oceanica: ecomorphological and functional correlates. *Marine Ecology Progress Series*, 163:267–278, 1998. doi: 10.3354/meps163267.

J. P. DeLong, J. G. Okie, M. E. Moses, R. M. Sibly, and J. H. Brown. Shifts in metabolic scaling, production, and efficiency across major evolutionary transitions of life. *Proceedings of the National Academy of Sciences*, 107(29):12941–12945, 2010. doi: 10.1073/pnas.1007783107.

J. Ding, B. Zhang, Y. Li, D. André, and O. Nilsson. Phytochrome b and phytochrome interacting factor8 modulate seasonal growth in trees. *New Phytologist*, 232(6):2339–2352, 2021. doi: 10.1111/nph.17350.

A. Emmaneel, K. Quintelier, D. Sichien, P. Rybakowska, C. Marañón, M. E. Alarcón-Riquelme, G. Van Isterdael, S. Van Gassen, and Y. Saeys. Peacoqc: Peak-based selection of high quality cytometry data. *Cytometry Part A*, 101(4):325–338, 2022. doi: 10.1002/cyto.a.24501.

M. Ermakova, C. Bellasio, D. Fitzpatrick, R. T. Furbank, F. Mamedov, and S. von Caemmerer. Upregulation of bundle sheath electron transport capacity under limiting light in c4 setaria viridis. *The Plant Journal*, 106(5):1443–1454, 2021. doi: 10.1111/tpj.15247.

P. Flombaum, J. L. Gallegos, R. A. Gordillo, J. Rincón, L. L. Zabala, N. Jiao, D. M. Karl, W. K. W. Li, M. W. Lomas, D. Veneziano, C. S. Vera, J. A. Vrugt, and A. C. Martiny. Present and future global distributions of the marine cyanobacteria prochlorococcus and synechococcus. *Proceedings of the National Academy of Sciences*, 110(24):9824–9829, 2013. doi: 10.1073/pnas.1307701110.

M. Geisler, D. J. Gibson, K. Lindsey, K. D. L. Millar, and A. J. dWood. Upregulation of photosynthesis genes, and downregulation of stress defense genes, is the response of arabidopsis thaliana shoots to intraspecific competition. *Botanical Studies*, 53:85–96, 2012. URL `https://api.semanticscholar.org/CorpusID:59376723`.

J. P. Gibert, Z.-Y. Han, D. J. Wieczynski, S. Votzke, and A. Yammine. Feedbacks between size and density determine rapid eco-phenotypic dynamics. *Functional Ecology*, 36(7):1668–1680, 2022. doi: 10.1111/1365-2435.14070.

S. K. Hoi, B. N. R. Winayu, H. T. Hsueh, and H. Chu. Light factors and nitrogen availability to enhance biomass and c-phycocyanin productivity of *Thermosynechococcus* sp. cl-1. *Biochemical Engineering Journal*, 167:107899, 2021. doi: 10.1016/j.bej.2020.107899.

J. Huisman, A. M. Johansson, E. O. Folmer, and F. J. Weissing. Towards a solution of the plankton paradox: The importance of physiology and life history. *Ecology Letters*, 4(5):408–411, 2001. doi: 10.1046/j.1461-0248.2001.00256.x.

R. Koch, A. Kupczok, K. Stucken, et al. Plasticity first: molecular signatures of a complex morphological trait in filamentous cyanobacteria. *BMC Evolutionary Biology*, 17:209, 2017. doi: 10.1186/s12862-017-1053-5.

D. Krause-Jensen and K. Sand-Jensen. Light attenuation and photosynthesis of aquatic plant communities. *Limnology and Oceanography*, 43(3):396–407, 1998. doi: 10.4319/lo.1998.43.3.0396.

E. Krichen, J. Harmand, M. Torrijos, J. J. Godon, N. Bernet, and A. Rapaport. High biomass density promotes density-dependent microbial growth rate. *Biochemical Engineering Journal*, 130:66–75, 2018. doi: 10.1016/j.bej.2017.11.017.

M. Kumar, J. Kulshreshtha, and G. P. Singh. Growth and biopigment accumulation of cyanobacterium *Spirulina platensis* at different light intensities and temperature. *Brazilian Journal of Microbiology*, 42:1128–1135, 2011. doi: 10.1590/S1517-83822011000300034.

T. Lamparter, F. Mittmann, W. Gärtner, T. Börner, E. Hartmann, and J. Hughes. Characterization of recombinant phytochrome from the cyanobacterium *Synechocystis*. *Proc Natl Acad Sci U S A*, 94(22):11792–11797, 1997. doi: 10.1073/pnas.94.22.11792.

T. J. Layden, C. T. Kremer, D. L. Brubaker, M. A. Kolk, J. V. Trout-Haney, D. A. Vasseur, and S. B. Fey. Thermal acclimation influences the growth and toxin production of freshwater cyanobacteria. *Limnology and Oceanography*, 7:34–42, 2022. doi: 10.1002/lol2.10197.

A. M. Leroi, A. F. Bennett, and R. E. Lenski. Temperature acclimation and competitive fitness: an experimental test of the beneficial acclimation assumption. *Proceedings of the National Academy of Sciences*, 91(5):1917–1921, 1994. doi: 10.1073/pnas.91.5.1917.

S. F. M. Levin, Bruce R. and L. Chao. Resource-limited growth, competition, and predation: A model and experimental studies with bacteria and bacteriophage. *The American Naturalist*, 111 (977):3–24, 1977. doi: 10.1086/283134.

Z.-P. Mei, Z. V. Finkel, and A. J. Irwin. Light and nutrient availability affect the size-scaling of growth in phytoplankton. *Journal of Theoretical Biology*, 259(3):582–588, 2009. doi: 10.1016/j.jtbi.2009.04.018.

G. Minotta and S. Pinzauti. Effects of light and soil fertility on growth, leaf chlorophyll content and nutrient use efficiency of beech (*Fagus sylvatica* l.) seedlings. *Forest Ecology and Management*, 86(1-3):61–71, 1996. doi: 10.1016/S0378-1127(96)03796-6.

M. Muramatsu and Y. Hihara. Acclimation to high-light conditions in cyanobacteria: from gene expression to physiological responses. *Journal of Plant Research*, 125:11–39, 2012. doi: 10.1007/s10265-011-0454-6.

J. O. Nalley, D. R. O'Donnell, and E. Litchman. Temperature effects on growth rates and fatty acid content in freshwater algae and cyanobacteria. *Algal Research*, 35:500–507, 2018. doi: 10.1016/j.algal.2018.09.018.

H. Ohkawa, C. Takatsuka, and T. Kawano. Hidden allee effect in photosynthetic organisms. *Communicative & Integrative Biology*, 13(1):119–127, 2020. doi: 10.1080/19420889.2020.1800999.

J. G. Okie. General models for the spectra of surface area scaling strategies of cells and organisms: Fractality, geometric dissimilitude, and internalization. *The American Naturalist*, 181(3):421–439, 2013. doi: 10.1086/669150.

O. Olusoji, J. Spaak, M. Holmes, T. Neyens, M. Aerts, and F. De Laender. cyanofilter: An r package to identify phytoplankton populations from flow cytometry data using cell pigmentation and granularity. *Ecological Modelling*, 460, Nov. 2021. ISSN 0304-3800. doi: 10.1016/j.ecolmodel.2021.109743.

H. Qiang, H. Guterman, and A. Richmond. Physiological characteristics of spirulina platensis (cyanobacteria) cultured at ultrahigh cell densities. *Journal of Phycology*, 32(6):1066–1073, 1996. doi: 10.1111/j.0022-3646.1996.01066.x.

A. Ramírez-Mata, I. J. Fernández-Domínguez, K. J. Nuñez-Reza, M. L. Xiqui-Vázquez, and B. E. Baca. Networks involving quorum sensing, cyclic-di-gmp, and nitric oxide on biofilm production in bacteria. *Rev Argent Microbiol*, 46(3):242–255, 2014. doi: 10.1016/s0325-7541(14)70079-3.

S. Raps, K. Wyman, H. W. Siegelman, and P. G. Falkowski. Adaptation of the cyanobacterium *Microcystis aeruginosa* to light intensity. *Plant Physiology*, 72(3):829–832, 1983. doi: 10.1104/pp.72.3.829.

B. Ren, W. Liu, J. Zhang, et al. Effects of plant density on the photosynthetic and chloroplast characteristics of maize under high-yielding conditions. *Scientific Reports*, 104(12), 2017. doi: 10.1007/s00114-017-1445-9.

R. Rippka, T. Coursin, W. Hess, C. Lichtle, D. J. Scanlan, K. A. Palinska, I. Iteman, and et al. Prochlorococcus marinus chisholm et al. 1992 subsp. pastoris subsp. nov. strain pcc 9511, the first axenic chlorophyll a2/b2-containing cyanobacterium (oxyphotobacteria). *International Journal of Systematic and Evolutionary Microbiology*, 50:1833–1847, 2000. doi: 10.1099/00207713-50-5-1833.

C. Six, J. Thomas, B. Brahamsha, Y. Lemoine, and F. Partensky. Photophysiology of the marine cyanobacterium *Synechococcus* sp. wh8102, a new model organism. *Aquatic Microbial Ecology*, 35(1):17–29, 2004. doi: 10.3354/ame035017.

J. W. Spaak and F. De Laender. Effects of pigment richness and size variation on coexistence, richness and function in light-limited phytoplankton. *Journal of Ecology*, 109(6):2385–2394, 2021. doi: 10.1111/1365-2745.13645.

I. N. Stadnichuk, P. M. Krasilnikov, and D. V. Zlenko. Cyanobacterial phycobilisomes and phycobiliproteins. *Microbiology*, 84:101–111, 2015. doi: 10.1134/S0026261715020150.

M. Stomp, J. Huisman, F. de Jongh, et al. Adaptive divergence in pigment composition promotes phytoplankton biodiversity. *Nature*, 432:104–107, 2004. doi: 10.1038/nature03044.

S.-F. Sui. Structure of phycobilisomes. *Annual Review of Biophysics*, 50(1):53–72, 2021. doi: 10.1146/annurev-biophys-062920-063657.

C. S. Ting, G. Rocap, J. King, and S. W. Chisholm. Cyanobacterial photosynthesis in the oceans: the origins and significance of divergent light-harvesting strategies. *Trends in Microbiology*, 10 (3):134–142, 2002. doi: 10.1016/S0966-842X(02)02319-3.

K. Trajkovic, C. Valdez, D. Ysselstein, and D. Krainc. Fluctuations in cell density alter protein markers of multiple cellular compartments, confounding experimental outcomes. *PLoS ONE*, 14 (2):e0211727, 2019. doi: 10.1371/journal.pone.0211727.

Y. Wang, R. Xie, Y. Shen, R. Cai, C. He, Q. Chen, W. Guo, Q. Shi, N. Jiao, and Q. Zheng. Linking microbial population succession and dom molecular changes in synechococcus-derived organic matter addition incubation. *Microbiol Spectr*, 10(2):e0230821, 2022. doi: 10.1128/spectrum.02308-21.

B. A. Ward, S. Dutkiewicz, O. Jahn, and M. J. Follows. A size-structured food-web model for the global ocean. *Limnology and Oceanography*, 57(6):1877–1891, 2012. doi: 10.4319/lo.2012.57.6.1877.

K. W. Wirtz. Non-uniform scaling in phytoplankton growth rate due to intracellular light and co2 decline. *Journal of plankton research*, 33(9):1325–1341, 2011. doi: 10.1093/plankt/fbr021.

J. Xie, S. Chen, and Z. Wen. Effects of light intensity on the production of phycoerythrin and polyunsaturated fatty acid by microalga *Rhodomonas salina*. *Algal Research*, 58:102397, 2021. doi: 10.1016/j.algal.2021.102397.

F. S. Xiong, E. C. Mueller, and T. A. Day. Photosynthetic and respiratory acclimation and growth response of antarctic vascular plants to contrasting temperature regimes. *American Journal of Botany*, 87(5):700–710, 2000. doi: 10.2307/2656856.

X. Zeng, M. Huang, Q.-X. Sun, Y.-J. Peng, X. Xu, Y.-B. Tang, J.-Y. Zhang, Y. Yang, and C.-C. Zhang. A c-di-gmp binding effector controls cell size in a cyanobacterium. *Proceedings of the National Academy of Sciences*, 120(13):e2221874120, 2023. doi: 10.1073/pnas.2221874120.

A Appendix

A.1 Supplemental methods

A.1.1 Light conditions

Figure S1 and Figure S2 : We measured light intensity with the SS-110 spectroradiometer and Launch ApogeeSpectrovision software from Apogee instruments. The device measured light intensity over a wavelength range from 340 to 820 nm. Light intensity was quantified via the photon flux density, expressed in μmol $m^{-2}s^{-1}nm^{-1}$. In addition to photosynthetic photon flux (PPF), the software also indicated the Yield Photon Flux (YPF), the Photosynthetic Photon Efficacy (PPE) and the ratio of red:far-red (R:FR). Full details of how to use the software can be found on the Apogee website. The measurements shown here are those taken when the spectroradiometer was in the middle of the incubator plate. In addition, we measured light intensities at various locations in the incubator to see whether light distribution in the incubator was homogeneous or heterogeneous. The amount of light distributed decreased as the spectroradiometer moved away from the LED axis. To avoid differences in light distribution between the plates, they were moved randomly every day after manipulation, ensuring that each plate did not end up in the same place where it had been the day before. Light intensity was lower in method 1 (46,97 μmol $m^{-2}s^{-1}nm^{-1}$) than in method 2 (79,77 μmol $m^{-2}s^{-1}nm^{-1}$).

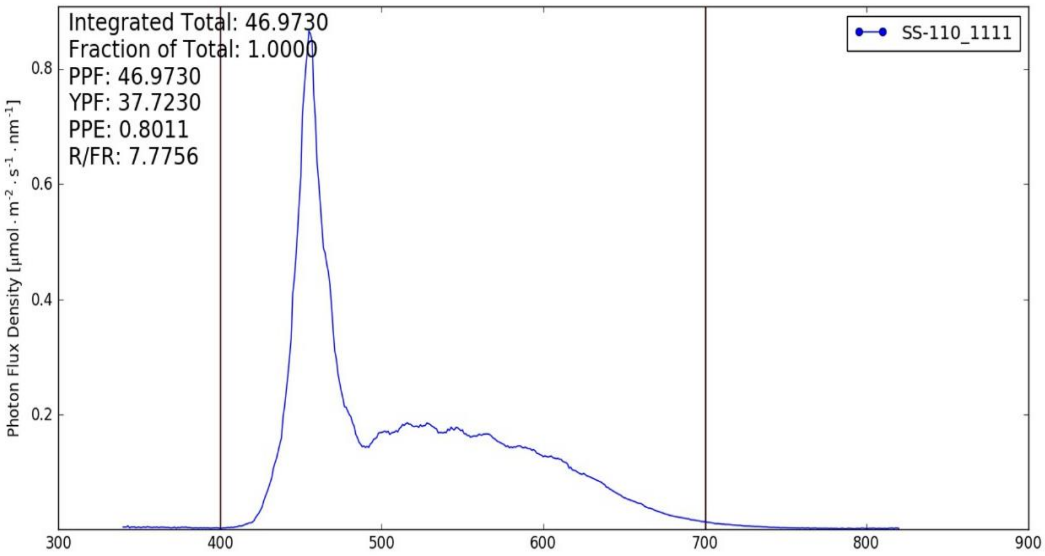

Figure S1: Light conditions in the incubator for method 1. The x-axis shows the wavelength in nanometres (nm) of the perceived light, ranging from 340 to 820 nm. The y-axis shows the flux photon density perceived by the spectroradiometer, expressed in μmol $m^{-2}s^{-1}nm^{-1}$. The light measurement was taken in the middle of the incubator. PPF : Photosynthetic Photon Flux, YPF : Yield Photon Flux, PPE : Photosynthetic Photon Efficacy, R:FR : Red to Far-Red Ratio.

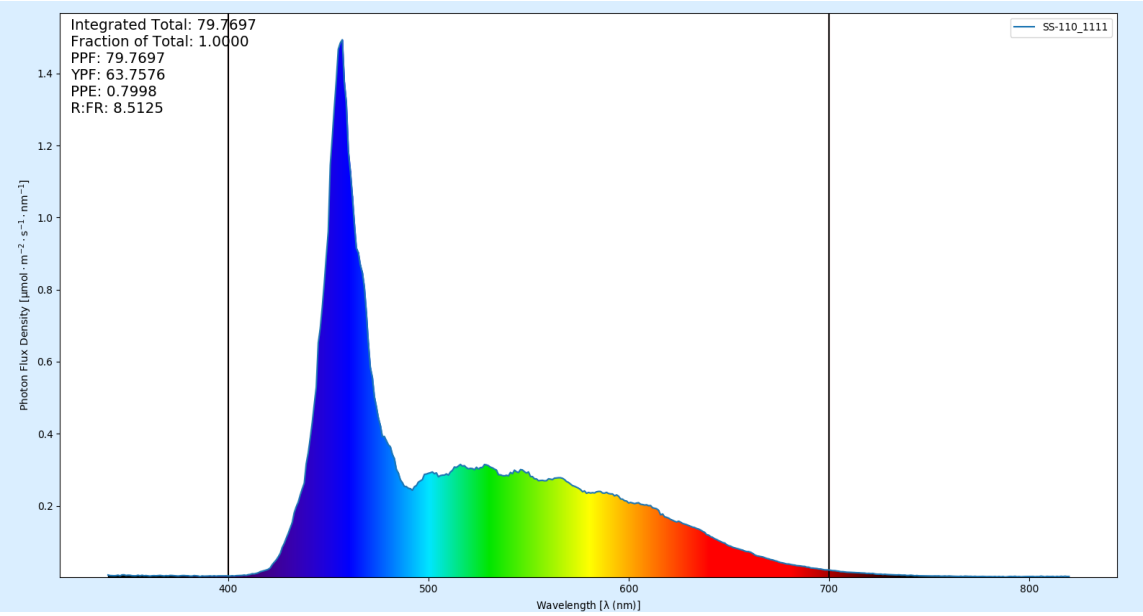

Figure S2: Light conditions in the incubator for method 2. For conditions of measurement, axis and abbreviations meanings, see Figure S1.

A.1.2 Experimental procedure

Figure S3 and Figure S4 illustrate the two phases of the experimental protocol. In the acclimation phase, to avoid the presence of clumps, we filtered the stock culture, which had been kept in an 100 mL Erlenmeyer under identical conditions as those of the experiment. We measured the density of this culture through flowcytometry (see A.2). Based on this density, we prepared an intermediate solution with a concentration of 75,000 cells μL^{-1}. From this culture, we inoculated two 6-well plates for each treatment with 2 mL of cultures and 4 mL of PCRS11 medium. Changes in density and traits were followed every day until the cultures reached distinct population sizes. The second phase started when the populations reached their final population densities. The replicates of a same treatment were mixed in an 100 mL Erlenmeyer. We measured the density of this solution. Based on this new stock cultures, we carried out several dilutions to obtain new densities of 10 000, 20 000, 35 000, 50 000, 90 000 (when possible) and 130 000 (when possible) cells μL^{-1} for the first experiment. In the second experiment, we diluted the cultures to obtain new densities of 15 000, 30 000, 50 000, 70 000, 100 000 (when possible) and 150 000 (when possible) cells μL^{-1}. We then measured the population densities for two days, enabling us to calculate the growth rate at the new dilutions.

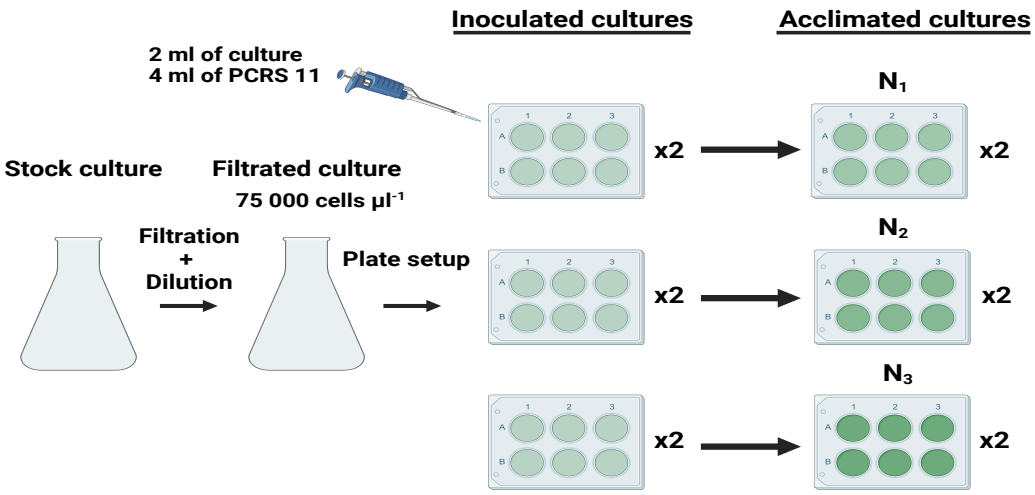

Figure S3: Acclimation phase protocol. Stock culture corresponds to the culture maintained in the laboratory. We filtrated and diluted this culture to obtain a new culture at 75 000 cells μL^{-1}. We then transferred 2ml of culture and 4mL of medium from this second culture to six 6-well plates, two plates per treatment. N_1, N_2 and N_3 correspond to the population densities reached at the end of the acclimation phase. Method 1 : $N_1 = 50\ 000$, $N_2 = 90\ 000$ and $N_3 = 130\ 000$ cells μL^{-1}. Method 2 : $N_1 = 80\ 000$, $N_2 = 130\ 000$ and $N_3 = 150\ 000$ cells μL^{-1}.

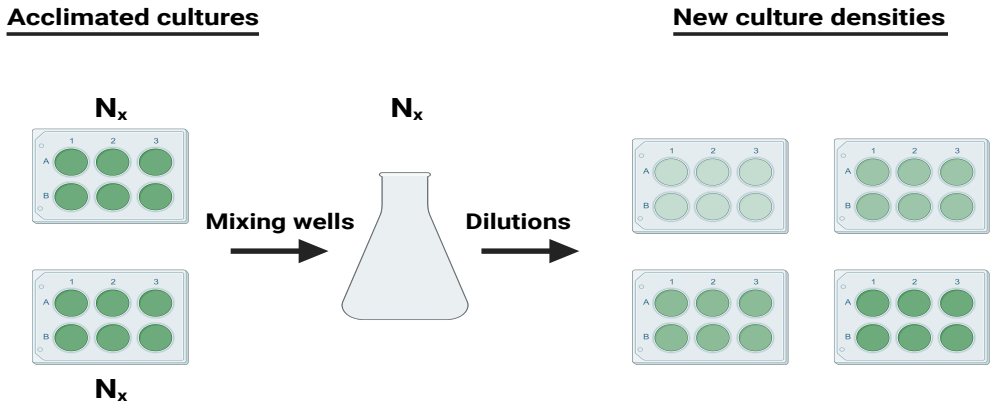

Figure S4: Space-for-time protocol. The figure shows the procedure for a single treatment only. Once a treatment achieved its final population density N_x, the replicates were mixed in an 100 mL Erlenmeyer. We then performed dilutions to obtain new densities. In method 1, new population densities were 10 000, 20 000, 35 000, 50 000, 90 000 (when possible) and 130 000 (when possible) cells μL^{-1}. In method 2, new populations densities were 15 000, 30 000, 50 000, 70 000, 100 000 (when possible) and 130 000 (when possible) cells μL^{-1}.

A.2 Cytometer measurement

Organisms' traits and populations densities were measured through flowcytometry. Every day, 200 μL of each well were sampled and transferred into some 96-well plates, one plate per treatment. Serial dilutions were performed so that our samples were in a concentration range from 50 to 500 cells μL^{-1}, being the range in which the cytometer can correctly measure the population density. To measure the population densities and the trait values, the cytometer detected optical and fluorescence signals using combination of lasers and detectors. These signal measurements were used as proxies of the cell morphology, with its size (Forward Scatter; FSC) and its internal complexity (Side Scatter; SSC) as well as three pigment contents : chlorophyll-a (RED.B, $\lambda = 488\,\text{nm}$), phycoerythrin (YEL.B, $\lambda = 488\,\text{nm}$) and phycocyanin (RED.R, $\lambda = 642\,\text{nm}$) (Adan et al., 2016). FSC light indicates the diffraction collected along the same axis as the laser beam, while SSC light is a measurement of refracted and reflected light, collected at approximately 90 degrees to the laser beam. These two signals are collected by photodiodes. RED.B, RED.R and YEL.B indicate the fluorescent emission resulting from pigment excitation by light beams. The cytometer counted 1000 cells for each well, recorded the data cell by cell and calculated the average value of the density and the traits. Dead cells, doublets and debris were removed using the CyanoFilter and PeacoQC packges in R version 4.3.1 (Emmaneel et al., 2022; Olusoji et al., 2021).

A.3 Supplemental results

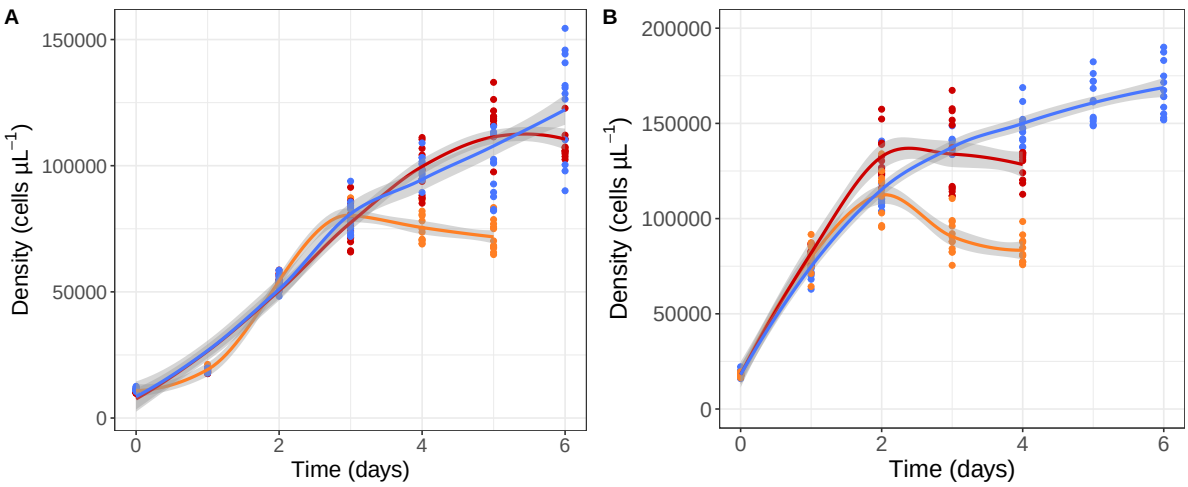

Figure S5: Density of cultures over time. Dots correspond to density values measured and smoothing curves represent overall trends of density over time. A : method of acclimation with dilutions when population reached their equilibrium. Orange : density_50 (n = 72), red : density_90 (n = 84), blue : density_130 treatment (n = 84). B : method of acclimation with a daily factor of dilution. Orange : density80 (n = 60), red : density130 (n = 60), blue : density170 treatment (n = 84).

Figure S5 : Density of cultures over time. In method 1, populations were diluted once they reached the desired concentrations in order to maintain them there. This method suffered from a lack of precision when it came to maintaining different acclimation densities. This may be one of the reasons why the density_90 and 130 treatments showed no significant difference in terms of concentration. In the method 2, populations reached higher final densities overall than in method 1. The method has made it possible to achieve the desired densities more precisely. The density80 underwent a large dilution (1/3), which explains its decrease already from the second day.

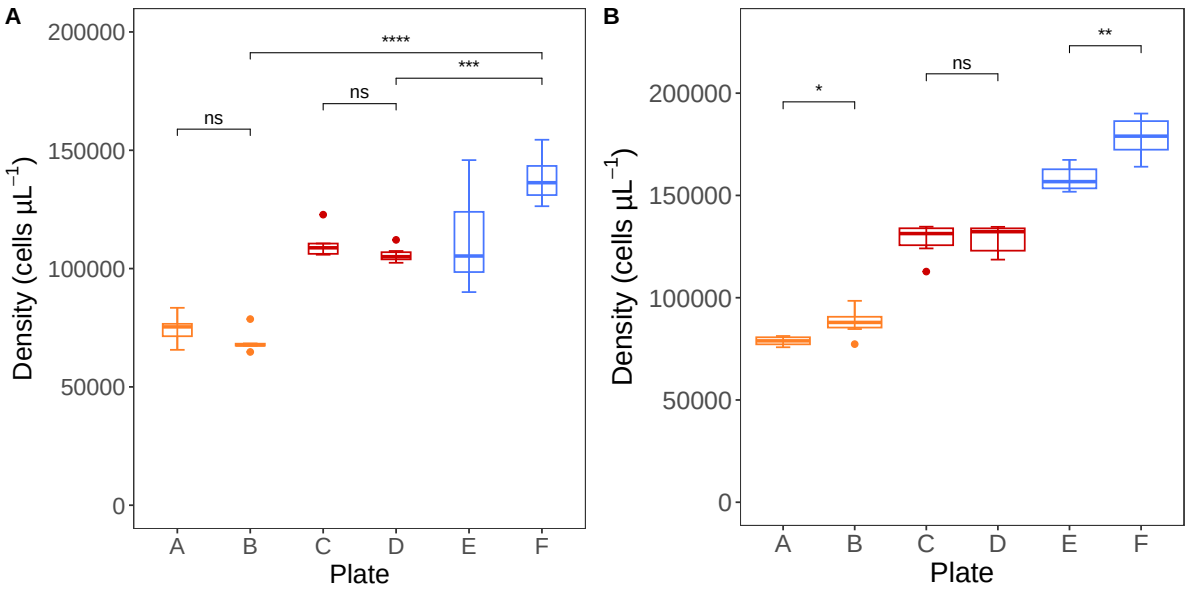

Figure S6: Final density for each plate. The figure shows median population densities (lines), 25% to 75% quartiles (boxes) and ranges (whiskers). Dots are shown if extreme values are more than 1.5 times the interquartile range of the box. For each plate, n = 6. A : method of acclimation with dilutions when population reached their equilibrium. Orange : density_50 (Plate A and B) , red : density_90 (Plate C and D) , blue : density_130 treatment (Plate E and F). B : method of acclimation with a daily factor of dilution. Orange : density80 (Plate A and B), red : density130 (Plate C and D), blue : density170 treatment (Plate E and F). * $p < 0.01$, ** $p < 0.001$, *** $p < 0.0001$.

Figure S6 : Final density of each plate. In method 1, the differences between the plate E and F, as well as the large variance of density values in the plate E, are both sources of explanations of non significant differences between the density_90 and the density_130 treatments. However, the F plate clearly reached a different density compared to the plates of the other treatments. This density in plate F was also the one expected for plate E. We were unable to determine the causes of this difference in density. A greater exposure to light at the end of the experiment for plate F or a better response to the dilutions applied are potential explanations. In method 2, some plates from a same treatment appeared to have significant different densities. However, these differences were still smaller than differences between treatments.

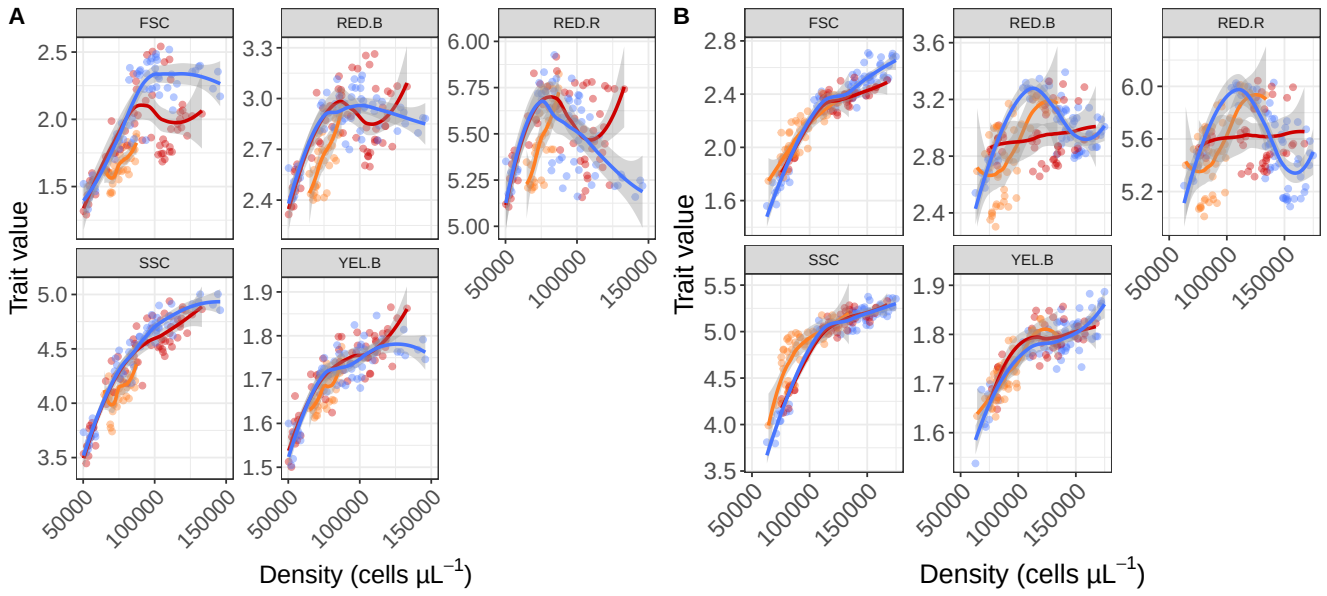

Figure S7: Mean trait values with density. Dot corresponds to mean trait values measured of replicates and smoothing curves represent the overall trends of traits with density. FSC : cell size, SSC : cell complexity, RED.B : chlorophyll-a content, YEL.B : phycoerythrin content and RED.R : phycocyanin content. A : method of acclimation with dilutions when population reached their equilibrium. Orange : density_50 (n = 72), red : density_90 (n = 84), blue : density_130 treatment (n = 84). B : method of acclimation with a daily factor of dilution. Orange : density80 (n = 60), red : density130 (n = 60), blue : density170 treatment (n = 84).

Figure S7: Mean trait values with density. In both methods, the traits reached different values from the start of the experiment and increased with density. The shape of the curves for certain traits, such as FSC, SSC and, to a lesser extent, YEL.B, followed those for density trends fairly closely. However, RED.B and RED.R evolved in a less clear and predictable way. Though they seemed to increase at first, the effect of density on the trait value changed according to the treatment and the method. This was reflected by the confidence interval around the smoothed regression curve increasing substantially after the end of the growing phase of RED.B and RED.R values, making it more complex to track value changes.

Table S1: Final trait values. FSC : cell size, SSC : cell complexity, RED.B : chlorophyll-a content, YEL.B : phycoerythrin content and RED.R : phycocyanin content.

	method 1				method 2			
FSC								
	Predictors	Estimates	CI	df	Predictors	Estimates	CI	df
	(Intercept)	1.64 ***	1.60 – 1.68	33	(Intercept)	1.93 ***	1.88 – 1.97	33
	density_90	0.13 ***	0.07 – 0.19	33	density130	0.40 ***	0.34 – 0.47	33
	density_130	0.72 ***	0.66 – 0.78	33	density170	0.67***	0.61 – 0.73	33
	Observations	36			Observations	36		
	R^2/R^2 adjusted	0.957 / 0.954			R^2/R^2 adjusted	0.939 / 0.935		
SSC								
	Predictors	Estimates	CI	df	Predictors	Estimates	CI	df
	(Intercept)	4.13 ***	4.06 – 4.19	33	(Intercept)	4.82 ***	4.77 – 4.88	33
	density_90	0.42 ***	0.33 – 0.51	33	density130	0.31 ***	0.23 – 0.40	33
	density_130	0.72 ***	0.63 – 0.81	33	density170	0.43 ***	0.34 – 0.51	33
	Observations	36			Observations	36		
	R^2/R^2 adjusted	0.888 / 0.882			R^2/R^2 adjusted	0.777 / 0.764		
RED.B								
	Predictors	Estimates	CI	df	Predictors	Estimates	CI	df
	(Intercept)	2.50 ***	2.46 – 2.55	33	(Intercept)	2.43 ***	2.39 – 2.47	33
	density_90	0.20 ***	0.13 – 0.26	33	density130	0.33 ***	0.28 – 0.39	33
	density_130	0.36 ***	0.30 – 0.43	33	density170	0.49 ***	0.43 – 0.54	33
	Observations	36			Observations	36		
	R^2/R^2 adjusted	0.791 / 0.778			R^2/R^2 adjusted	0.904 / 0.898		
YEL.B								
	Predictors	Estimates	CI	df	Test	χ^2	df	
	(Intercept)	1.65 ***	1.63 – 1.67	33	Kruskal-Wallis	26.668***	2	
	density_90	0.09 ***	0.07 – 0.12	33				
	density_130	0.10 ***	0.08 – 0.13	33				
	Observations	36						
	R^2/R^2 adjusted	0.744 / 0.728						
RED.R								
	Test	χ^2	df	Test	χ^2	df		
	Kruskal-Wallis	0.06374	2	Kruskal-Wallis	18.893***	2		
	* p<0.05	** p<0.01	*** p<0.001					

Table S1 : Final trait values. In both methods, populations acclimated to higher densities exhibited higher FSC and SSC values. R^2 and R^2 adjusted were high, especially for FSC models. For FSC, when comparing treatment from similar densities but from different methods (e.g. density_130 from method 1 and density130 from method 2), values were quite equivalent. However, for SSC, treatments of method 2 exhibited higher mean values than treatments of method 1 with similar densities. For RED.B, populations acclimated to higher densities showed significantly higher RED.B contents. R^2 and R^2 adjusted were quite higher in the method 2 compared to the method 1. For YEL.B in method 1, every treatment showed significant differences in values. However, these differences were much smaller than with the other traits, which might suggest that this trait has a fairly stable content. In method 2, heteroscedasticity prevented from ANOVA tests. However, a kruskal Wallis test showed a global difference in YEL.B values between treatments. For RED.R, heteroscedasticity also prevented us from performing ANOVA tests. Kruskal Wallis tests yet showed significant differences in method 2 but not in method 1.

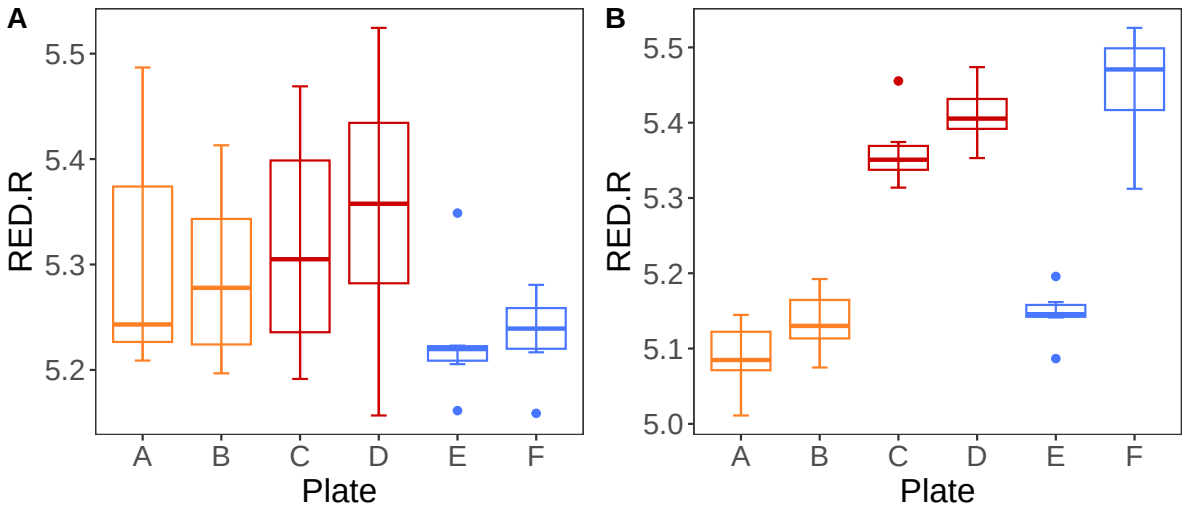

Figure S8: Final RED.R values for each plate. The figure shows median RED.R values(lines), 25% to 75% quartiles (boxes) and ranges (whiskers). Dots are shown if extreme values are more than 1.5 times the interquartile range of the box. For each plate, n = 6. A : method of acclimation with dilutions when population reached their equilibrium. Orange : density_50 (Plate A and B) , red : density_90 (Plate C and D) , blue : density_130 treatment (Plate E and F). B : method of acclimation with a daily factor of dilution. Orange : density80 (Plate A and B), red : density130 (Plate C and D), blue : density170 treatment (Plate E and F).

Figure S8 : Final RED.R values for each plate. In method 1, both density_50 and density_90 treatments showed large variation within their plates. In method 2, the high variation in the density170 treatment was mainly explained by the large differences in RED.R values between plates. This difference between the two plates can be due to the difference in density. However it is unlikely that it is the only factor influencing this difference in RED.R values. It is possible that one of the plates was exposed to more light than the other at the end of the experiment.

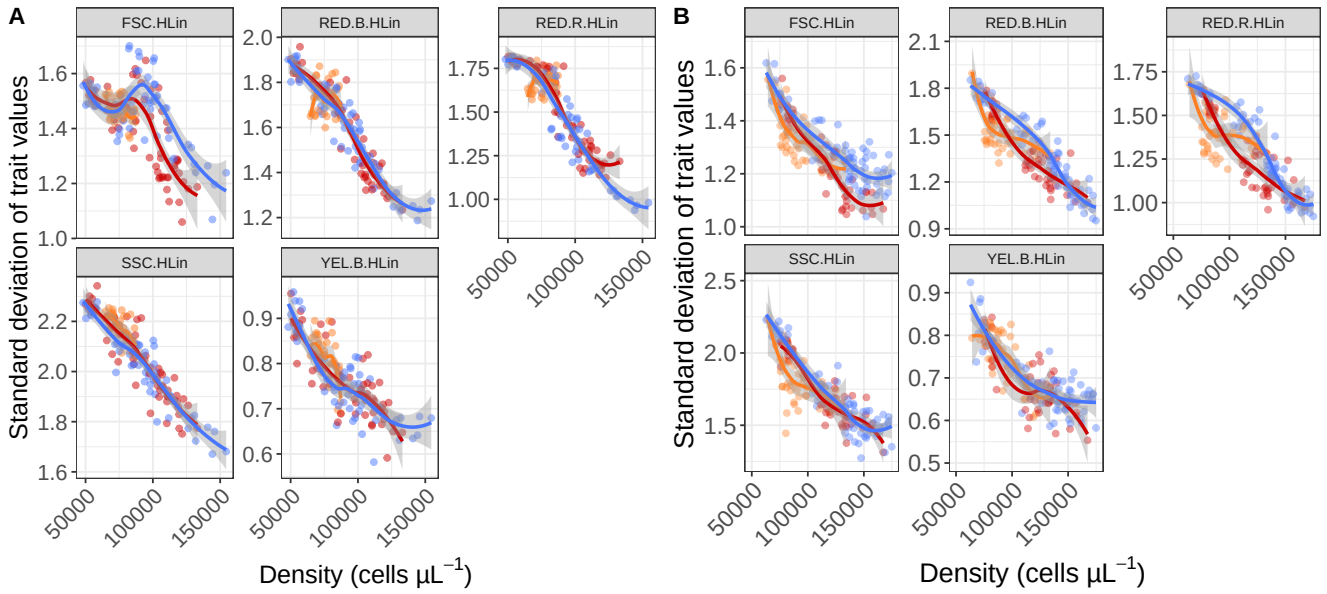

Figure S9: Standard deviation of trait values with density. Dots correspond to the standard deviation of traits within replicates and smoothing curves represent the overall trends of trait standard deviation over time. For AB, abbreviations and colour meanings, see Supplements, Fig. S7.

Figure S9 : Standard deviation of trait values with density. The standard deviation of each trait decreased with density linearly, except for FSC in method 1. When comparing the variability of each trait between the two methods, they showed fairly similar valuess. YEL.B exhibited an intrinsic lower standard deviation than the other traits.

Table S2: Final standard deviation of traits for each plate in method 1. FSC : cell size, SSC : cell complexity, RED.B : chlorophyll-a content, YEL.B : phycoerythrin content and RED.R : phycocyanin content.

	Contrast	estimate	Std.Error	t.ratio	df
FSC	A - B	0.023	0.032	0.733	25
	B - D	0.269 ***	0.032	8.254	25
	C - D	0.020	0.032	0.636	25
	B - F	0.249 ***	0.032	7.638	25
	D - F	-0.02	0.032	-0.616	25
RED.R	A - B	-0.014	0.026	-0.537	25
	B - D	0.363 ***	0.026	13.502	25
	C - D	-0.029	0.026	-1.111	25
	B - F	0.614 ***	0.026	22.839	25
	D - F	0.251 ***	0.026	9.337	25
YEL.B	A - B	-0.027	0.020	-1.339	25
	B - D	0.103 ***	0.020	5.035	25
	C - D	-0.028	0.020	-1.406	25
	B - F	0.198 ***	0.020	9.660	25
	D - F	0.094 **	0.020	4.625	25
SSC	A - B	0.0108	0.024	0.445	25
	B - D	0.28 ***	0.024	11.499	25
	C - D	0.003	0.024	0.147	25
	B - F	0.468 ***	0.024	19.192	25
	D - F	0.187 ***	0.024	7.692	25

* p<0.05 ** p<0.01 *** p<0.001

Table S2 : Final standard deviation of traits for each plate in method 1. Contrasts methods with Bonferonni correction were performed to compare trait standard deviations between plates. Plate E was removed because of large variance, leading to problems of heteroscedasticity. There was never significant differences between two plates of a same treatment. However, for every trait except FSC (Plate D and F), two plates from different treatments always exhibited standard deviations that were significantly different from each other.

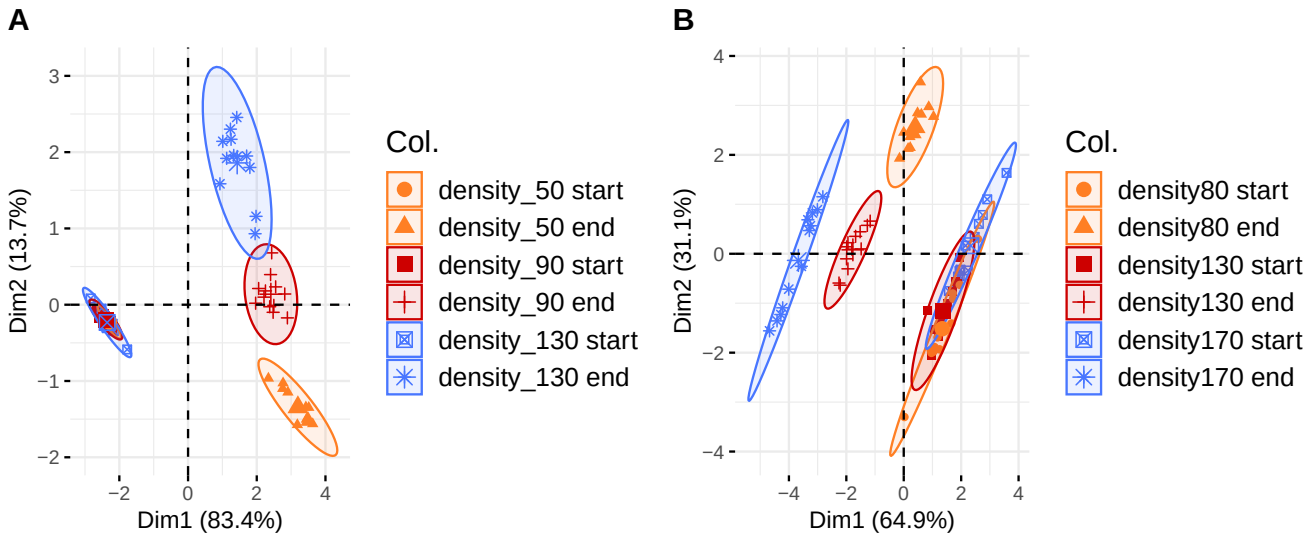

Figure S10: PCA analysis on cultures at the start and the end of the acclimation phase. For each treatment at the start or at the end of the experiment, n = 12. A : method of acclimation with dilutions when population reached their equilibrium. Orange : density_50, red : density_90, blue : density_130 treatment. B : method of acclimation with a daily factor of dilution. Orange : density80, red : density130, blue : density170 treatment.

Figure S10 : PCA analysis on cultures at the start and the end of the acclimation phase. The variables used were the trait values and the densities. In both methods, populations at the end of the acclimation phase were distinct from populations at the start of the acclimation phase. Every population at the end of the acclimation phase were also distinct from each other, despite a slight overlap between two treatments in method 1. The combination of both axis explained respectively 97,1 % and 96 % of the total variation in our culture for method 1 and 2, indicating that the variables used explained a significant proportion of the variation in our data.

Table S3: Density dependence of growth model for method 1.

			per-capita growth rate	
	Predictors	Estimates	Std.Error	t.value
Density_50	(Intercept)	6.119e-01 ***	4.505e-02	13.582
	poly(lag.dens, 1)	-1.338e-05 ***	2.244e-06	-5.963
	Observations	12		
	df	10		
	R^2/R^2 adjusted	0.780 / 0.759		
Density_90	(Intercept)	-1.097e-01	1.041e-01	-1.054
	poly(lag.dens, 3)1	3.836e-05 ***	7.970e-06	4.813
	poly(lag.dens, 3)2	-7.950e-10 ***	1.586e-10	-5.014
	poly(lag.dens, 3)3	4.364e-15 ***	9.188e-16	4.750
	density_130	9.46e-02 *	3.709e-02	2.551
	Observations	33		
	df	28		
	R^2/R^2 adjusted	0.696 / 0.6531		
	* p<0.05	** p<0.01	*** p<0.001	

Table S3 : Density dependence of growth model for method 1. For every treatment, polynomial models of different degrees were compared. The models shown here were those with the best AIC. Overall, models fitted the data fairly well, with minimum R^2 adjusted values of 65% amounting up to 76%. The density_50 treatment was best fitted to a linear regression, while the two other treatments were best fitted to a polynomial model of a degree 3. When comparing the two models of a degree 3, the density_130 had a significant higher intrinsic growth rate than the density_90 treatment. The density_90 treatment even showed a negative intrinsic growth rate, suggesting a strong Allee effect.

Table S4: Density dependence of growth model for method 2.

			per-capita growth rate	
	Predictors	Estimate	Std. Error	t value
Density80	(Intercept)	2.526e-01 ***	1.363e-02	18.527
	lag.dens	-2.656e-06 ***	5.440e-07	-4.479
	treatdensity130	5.567e-02 **	5.227e-02	3.286
	lag.dens:treatdensity130	8.929e-07 **	2.655e-07	3.363
	Observations	33		
	df	29		
	R^2/R^2 adjusted	0.921 / 0.913		
Density 170	(Intercept)	-7.427e-01 ***	1.215e-01	-6.111
	poly(lag.dens, 4)1	7.485e-05 ***	8.173e-06	9.158
	poly(lag.dens, 4)2	-1.585e-09 ***	1.692e-10	-9.368
	poly(lag.dens, 4)3	1.266e-14 ***	1.383e-15	9.150
	poly(lag.dens, 4)4	-3.442e-20 ***	3.892e-21	-8.845
	Observations	18		
	df	13		
	R^2/R^2 adjusted	0.937 / 0.918		
	* p<0.05	** p<0.01	*** p<0.001	

Table S4 : Density dependence of growth model for method 2. For every treatment, polynomial models of different degrees were compared. The models shown here were those with the best AIC. Both density80 and density130 were best fitted to linear regressions. The interaction between the density and the treatment variable was significant, indicating a significant effect of the density acclimation treatment on the slope, reflecting the density dependence. The slope was steeper for the density80, indicating a higher density dependence. This treatment also exhibited a significantly lower intrinsic growth rate compared to density130 treatment. The model explained much of the variation in the data (R^2 = 92,1%). The highest density treatment showed a polynomial regression of a degree 4. The y-intercept was quite low, suggesting a strong Allee effect. The model also explained much of the variation in the data (R^2 = 93,7 %).

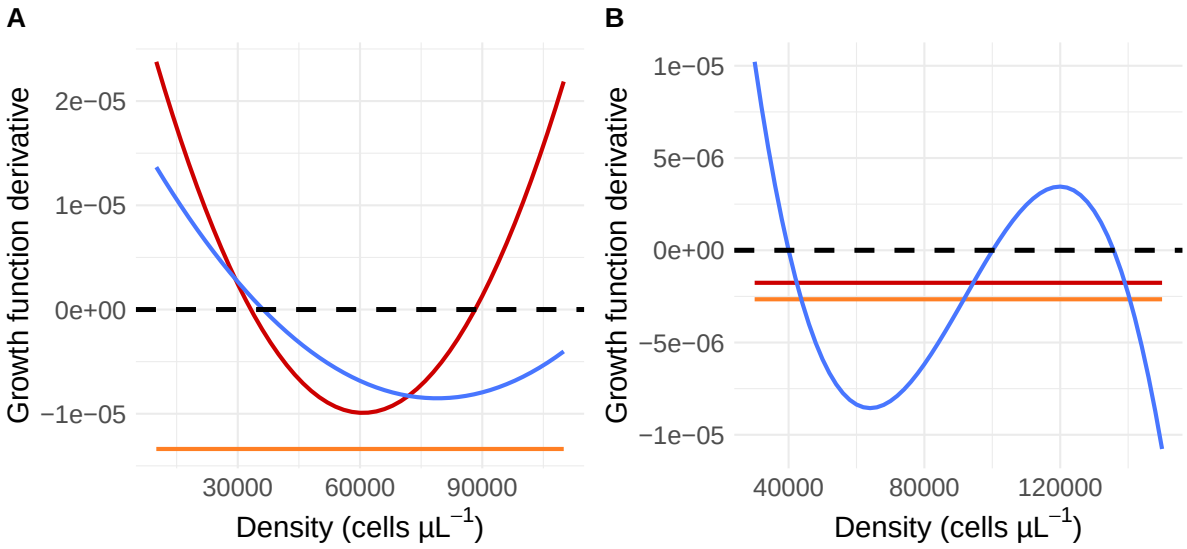

Figure S11: Derivatives of the estimated growth functions. Curves correspond to the derivatives of the estimated functions of population growth. Horizontal dashed line indicates the abcissa of the graph. A : method of acclimation with dilutions when population reached their equilibrium. Orange : density_50, red : density_90, blue : density_130 treatment. B : method of acclimation with a daily factor of dilution. Orange : density80, red : density130, blue : density170 treatment.

Figure S11 : Derivatives of the estimated growth functions. We performed the derivative of each growth function to better analyze the density dependence of different treatments based on population density. In method 1, we observed, for the density_90 and 130 treatments, that density dependence was positive up to approximately a population density of 35,000 cells μL^{-1}. This positive density dependence was more pronounced for the density_90 treatment up to 30,000 cells μL^{-1}, which is approximately the final density where treatments exhibited positive density dependence. As the densities of the treatments became negative, the density_90 treatment showed more strongly negative values than those of the density_130 treatment up to around 75,000 cells μL^{-1}, indicating that density dependence was more significant in density_90. This relationship reversed after the population density exceeded 75,000 cells μL^{-1}. In method 2, density80 treatment showed a more negative value than density130 treatment, indicating a higher density dependence. Density170 showed a positive derivative up to a density of 40,000 cells/μL and also between 100,000 and almost 140,000 cells μL^{-1}. The minimum value was at around 60,000 cells μL^{-1} and the optimum value was at around 120 000 cells μL^{-1}.